Journal of Virology

Virology | Full-Length Text

Stabilization of the human cytomegalovirus UL136p33 reactivation determinant overcomes the requirement for UL135 for replication in hematopoietic cells

Melissa A. Moy,[1,2,3] Donna Collins-McMillen,[2,3] Lindsey Crawford,[4] Christopher Parkins,[4] Sebastian Zeltzer,[2,3] Katie Caviness,[2,3,5] Syed Shujaat Ali Zaidi,[2] Patrizia Caposio,[4] Felicia Goodrum[1,2,3,5]

AUTHOR AFFILIATIONS See affiliation list on p. 19.

ABSTRACT Human cytomegalovirus (HCMV) is a beta herpesvirus that persists indefinitely in the human host through a latent infection. The polycistronic *UL133–UL138* gene locus of HCMV encodes genes regulating latency and reactivation. While *UL138* is pro-latency, restricting virus replication in CD34$^+$ hematopoietic progenitor cells (HPCs), *UL135* overcomes this restriction and is required for reactivation. By contrast, *UL136* is expressed with later kinetics and encodes multiple proteins with differential roles in latency and reactivation. Like *UL135*, the largest *UL136* isoform, UL136p33, is required for reactivation from latency in HPCs; viruses failing to express either protein are unresponsive to reactivation stimuli. Furthermore, UL136p33 is unstable, and its instability is important for the establishment of latency, and sufficient accumulation of UL136p33 is a checkpoint for reactivation. We hypothesized that stabilizing UL136p33 might overcome the requirement of *UL135* for replication. We generated recombinant viruses lacking *UL135* that expressed a stabilized variant of UL136p33. Stabilizing UL136p33 did not impact the replication of the *UL135* mutant virus in fibroblasts. However, in the context of infection in HPCs, stabilization of UL136p33 strikingly compensated for the loss of *UL135*, resulting in increased replication in CD34$^+$ HPCs and in humanized NOD-*scid* IL2Rγ_c^{null} (huNSG) mice. This finding suggests that while *UL135* is essential for replication in HPCs, it functions largely at steps preceding the accumulation of UL136p33, and that stabilized expression of UL136p33 largely overcomes the requirement for *UL135*. Taken together, our genetic evidence indicates an epistatic relationship between UL136p33 and *UL135*, whereby *UL135* may initiate events early in reactivation that drive the accumulation of UL136p33 to a threshold required for productive reactivation.

IMPORTANCE Human cytomegalovirus (HCMV) is one of nine human herpesviruses and a significant human pathogen. While HCMV establishes a lifelong latent infection that is typically asymptomatic in healthy individuals, its reactivation from latency can have devastating consequences in the immunocompromised. Defining viral genes important in the establishment of or reactivation from latency is important to defining the molecular basis of latent and replicative states and in controlling infection and CMV disease. Here we define a genetic relationship between two viral genes in controlling virus reactivation from latency using primary human hematopoietic progenitor cells and humanized mouse models.

KEYWORDS cytomegalovirus, herpesvirus, latency, reactivation, *UL135*, *UL136*

The molecular programs by which herpesviruses persist in a latent state or reactivate for replication are poorly understood. DNA herpesviruses are a robust model for elucidating mechanisms of viral latency because of the complex virus–host interactions

Editor Anna Ruth Cliffe, University of Virginia, Charlottesville, Virginia, USA

Address correspondence to Felicia Goodrum, fgoodrum@arizona.edu.

The authors declare no conflict of interest.

See the funding table on p. 19.

Received 25 January 2023
Accepted 20 June 2023
Published 11 August 2023

that allow the virus to "sense" and "respond" to changes in host biology. Human cytomegalovirus (HCMV) is a large ~236 kb double-stranded DNA beta herpesvirus with a global seroprevalence of approximately 60% to 99% based on geographic and socioeconomic factors (1–3). Infection is typically asymptomatic in immunocompetent individuals. Once latency is established, subclinical sporadic reactivation and virus shedding can occur throughout the lifetime of the host (4, 5). For immunocompromised individuals with inadequate cellular immunity, reactivation from latency can result in morbidity and mortality, particularly in stem cell and solid organ transplant recipients (4–8). Further, congenital CMV infection can cause significant neurodevelopmental abnormalities, affecting approximately 1 in 150 babies born in the United States (9–15). HCMV infection may enhance immune responses in young adults but may be a driver in age-related pathologies and altered T cell homeostasis (16–18). Therefore, understanding the viral and host mechanisms underpinning HCMV persistence and reactivation is critical to developing strategies to control its reactivation and associated pathologies.

HCMV exhibits broad intra-host tropism. HCMV replicates productively in human primary fibroblasts and in epithelial and endothelial cells. HCMV latency has been best characterized in hematopoietic progenitor cells (HPCs; $CD34^+$ HPCs) and cells of the myeloid lineage (19). During latency, viral genomes are maintained, viral gene expression is restricted, and no new viral progeny are made. HCMV reactivates in response to viral and host cues, including cellular stress, inhibition of PI3K/Akt signaling, differentiation, or steroid treatment to re-initiate viral gene expression (4, 20–26). Viruses have evolved complex gene networks to sense and respond to multiple environmental stimuli that can feedback to impact viral gene expression (19, 27, 28).

The ~15 kb UL*b*′ region of the HCMV genome spans *UL133* to *UL150* and encodes genes important to the regulation of immune responses, viral persistence, and dissemination (4, 29–33). The UL*b*′ region is present in low-passage strains and clinical isolates but lost during serial passage of the virus in fibroblasts, thus partly or entirely lacking in most laboratory-adapted strains. While largely dispensable for replication in fibroblasts, these genes undoubtedly play important roles in other contexts of infection in the host (34–37). We have characterized a 3.6 kb polycistronic gene locus within the UL*b*′ region encoding four genes, *UL133, UL135, UL136,* and *UL138,* collectively referred to as the *UL133–UL138* locus (19, 38). On the whole, the *UL133–UL138* locus is suppressive to viral replication in HPCs (34, 35). Using recombinant viruses containing disruptions of a single gene or combinations of genes in this locus, we have defined genetic phenotypes for each gene with respect to the establishment of or reactivation from latency in hematopoietic cells. *UL138* is pro-latency in that genetic disruption of *UL138* allows HCMV to replicate in the absence of a reactivation stimulus and results in increased viral yields relative to the parental wild-type (WT) virus (34, 39). Conversely, *UL135* is pro-replication and necessary for reactivation from latency (40). UL135 functions, in part, to overcome the suppressive effect of UL138 for reactivation. Both *UL135* and *UL138* are expressed early, prior to the onset of viral DNA synthesis. *UL135* also has an epistatic relationship with the viral serine–threonine protein kinase, *UL97*, whereby *UL135* function confers a heightened requirement for *UL97* for viral DNA synthesis and viral gene expression in a productive infection (41). Although *UL97* is the only HCMV-encoded kinase, it is remarkably dispensable for replication in the laboratory-adapted strains lacking *UL135* (41, 42).

UL136 is a complex gene that encodes five proteins, referred to as isoforms, resulting from alternative transcription initiation start sites (43). *UL136* is expressed with early to late expression kinetics (43, 44), as maximal expression requires viral DNA synthesis, in contrast to other *UL133–UL138* locus genes that are expressed with delayed early kinetics. *UL136* and its protein isoforms are dispensable for replication in fibroblasts, but important for replication in microvascular endothelial cells. Further, *UL136* proteins have roles in both latency and reactivation. The UL136-33kDa (UL136p33) and UL136-26kDa (UL136p26) membrane-associated isoforms are required for reactivation, phenocopying a loss of *UL135* (44). The UL136-25kDa (UL136p25) isoform has context-dependent roles,

where disruption of this isoform results in a more replicative virus in HPCs infected *in vitro*, but a virus that fails to reactivate humanized mice (44). The UL136-23kDa (UL136p23) and UL136-19kDa (UL136p19) isoforms, which have not been separated genetically, are soluble and pro-latency. Similar to *UL138*, a virus that cannot express the UL136p23/19 isoforms replicates robustly in hematopoietic cells in the absence of a reactivation stimulus (43, 44). Given these early to late expression kinetics and the differential roles in latency and reactivation of the *UL136* isoforms, we postulate that *UL136* functions to toggle the balance between a *UL138*-dominant latent state and a *UL135*-dominant reactivated state in response to host cues.

We have recently defined an important regulatory checkpoint for controlling accumulation of the UL136p33 isoform for reactivation. UL136p33 is unstable relative to other *UL136* isoforms (45). We have further shown that the host E3 ubiquitin ligase, an inducible degrader of low-density lipoprotein receptor (IDOL, also known as MYLIP), targets UL136p33 for rapid proteasomal degradation (45). When UL136p33 is stabilized, HCMV is more replicative in the absence of a reactivation stimulus in $CD34^+$ HPCs. IDOL is highly expressed in undifferentiated hematopoietic cells, but is downregulated sharply upon differentiation. Consistent with a role for IDOL-mediated regulation of UL136p33 for latency, induction of IDOL during infection in $CD34^+$ HPCs restricts replication, whereas knockdown of IDOL increases virus gene expression in hematopoietic models. This work demonstrates the importance of UL136p33 instability for the establishment of latency and defines a key cellular pathway regulating UL136p33 levels and HCMV fate decisions with regard to entry into and exit from latency (45).

The independent requirements for *UL135* and UL136p33 for reactivation from latency along with their sequential temporal expression pattern suggest an epistatic relationship between *UL135* and *UL136* genes for controlling latency and reactivation. We hypothesized that stabilizing UL136p33 might obviate the need for *UL135* for replication in hematopoietic cells if, for example, *UL135* initiated events in infection that resulted in the accumulation of UL136p33. To explore the possible interdependence between *UL135* and UL136p33 for HCMV reactivation and replication, we generated *UL136* recombinant viruses where UL136p33 was stabilized in the presence or absence of *UL135*. We demonstrate here that stabilizing UL136p33 does not compensate for the modest defects resulting from the loss of *UL135* in fibroblasts. However, in a latent infection, stabilization of UL136p33 strikingly compensates for the loss of *UL135*, resulting in enhanced virus replication (a failure to establish latency) and genome amplification. Importantly, this phenotype is recapitulated in humanized NSG (huNSG) mice. Taken together, our evidence suggests an epistatic relationship between UL136p33 and *UL135* for controlling HCMV reactivation from latency, where *UL135* is dispensable for replication in $CD34^+$ HPCs when UL136p33 expression is ensured.

RESULTS

Stabilizing UL136p33 modestly alters viral gene expression in a productive infection

We have previously shown that *UL135* exhibits early expression kinetics, while *UL136* isoforms exhibit early to late expression kinetics in a productive infection in fibroblasts (43) and that UL136p33 is unstable and its accumulation is required for reactivation (45). Further, as *UL135* and UL136p33 are both required for reactivation from latency, we hypothesized an epistatic relationship whereby UL135 function may drive aspects of infection required for the accumulation of UL136p33 at late times. If true, then stabilizing UL136p33 might overcome the requirement for *UL135* for replication. UL136p33 is stabilized by the substitution of four lysine residues for arginine, $UL136_{myc}\Delta K{\rightarrow}R$. To investigate the possible relationship between *UL135* and UL136p33, we generated recombinant bacterial artificial chromosomes (BAC) by substituting *UL136* variants encoding the C-terminal myc epitope-tagged version of *UL136*, $UL136_{myc}$, or the stabilized version of *UL136*, $UL136_{myc}\Delta K{\rightarrow}R$, into a previously characterized $\Delta UL135_{STOP}$ bacterial artificial chromosome (BAC) where *UL135* expression is disrupted by the

insertion of stop codons (43, 45). The myc epitope tag is required to detect *UL136* as we have been unsuccessful in generating antibodies to *UL136* despite multiple attempts. Further, while UL136 is important for infection in hematopoietic cells as defined by the phenotypes associated with disruption of specific isoforms or combinations of isoforms (43, 44), *UL136* is expressed at such low levels in $CD34^+$ HPCs that we have not been able to detect protein even with the myc epitope tag. A schematic of the recombinant viruses used in this study is shown in Fig. 1A. Whole-genome sequencing was performed to ensure mutations were located at the desired positions on the viral genome and that recombination did not affect other regions of the genome (Fig. 1B). In addition, a schematic of the specific nucleotides that were mutated is specified for each recombinant virus (Fig. 1C).

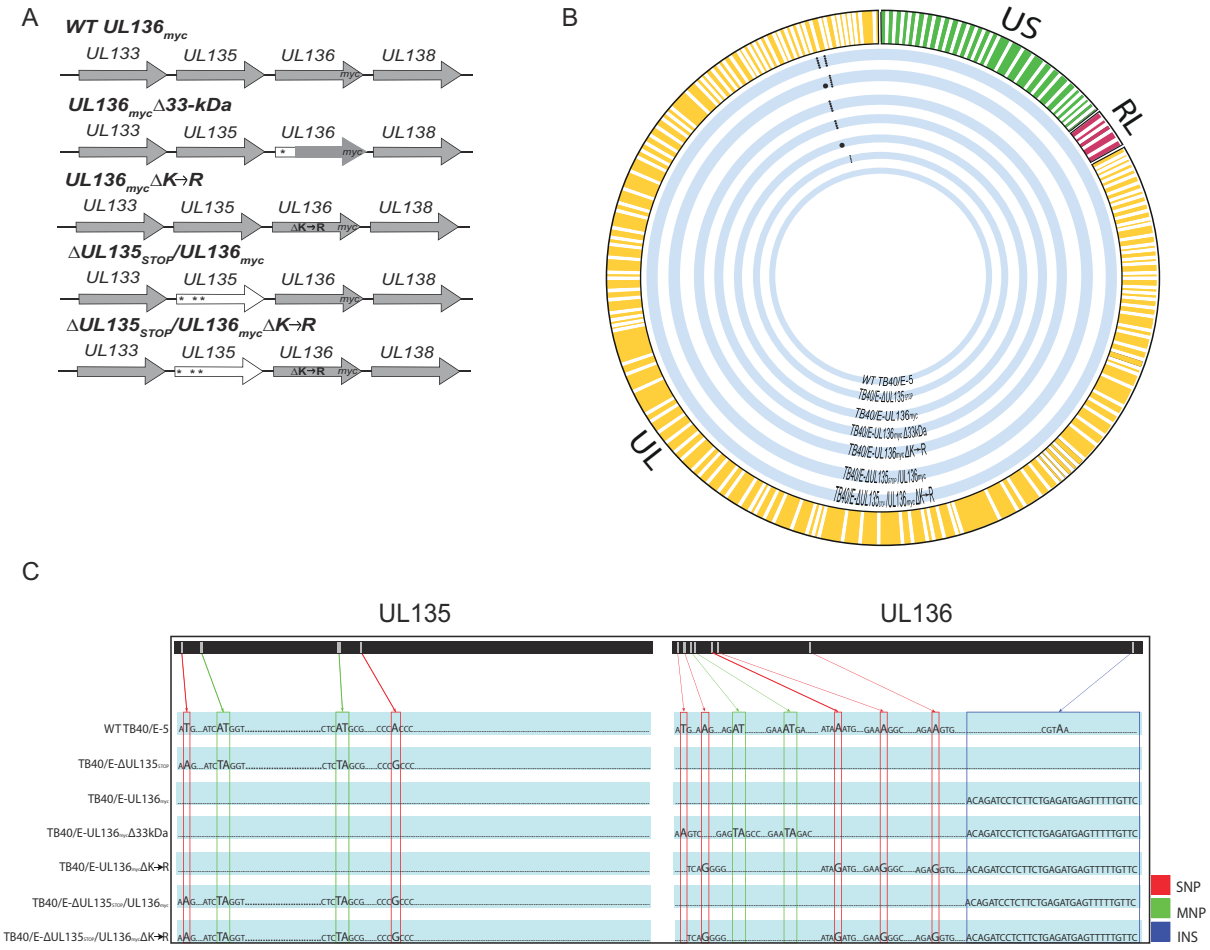

FIG 1 Schematic and whole-genome sequencing of viruses used in this study. (A) Schematic of changes within the *UL133–UL138* locus in TB40/E recombinant viruses indicated. Parental (WT) $UL136_{myc}$ expresses *UL136* fused in frame with a C-terminal *myc* epitope tag. All recombinant viruses used in this study are derived from this virus and express the myc epitope-tagged version of *UL136* for protein detection. $UL136_{myc}$*Δ33kDa* contains stop codon substitutions for 5′ AUGs to disrupt the expression of UL136p33. $UL136_{myc}$*ΔK→R* contains arginine substitutions for all four lysine residues in *UL136* (amino acid positions 4, 20, 25, and 113). $\Delta UL135_{STOP}/\Delta UL136_{myc}$ contains stop codon substitutions for 5′ AUGs to abrogate synthesis of UL135 protein (amino acid positions 1, 27, and 97). $\Delta UL135_{STOP}/\Delta UL136_{myc}\Delta K{\rightarrow}R$ combines the stop codon substitutions in *UL135* with the lysine to arginine substitutions in *UL136* described above. * indicates stop codon substitutions for methionine codons. (B) Whole-genome sequencing and alignment of parental (TB40/E) and recombinant HCMV bacterial artificial chromosomes (BACs) was performed to identify alterations in each recombinant virus. Thick blue lines represent each recombinant virus as labeled, and mutations in each genome are denoted by black dots. (C) Zoomed in pictograph of *UL135* and *UL136* genes with specific nucleotide changes evident in sequencing. Single-nucleotide polymorphisms (SNPs) are boxed in red; multiple nucleotide polymorphisms (MNPs) are boxed in green; and insertions (INS) are boxed in blue. Mutations for each recombinant virus are compared back to the WT TB40/E-5 parental virus.

We first characterized viral gene expression during infection in MRC-5 fibroblasts. Fibroblasts support only a replicative infection and are a foundational model in the field for understanding HCMV replication. While *UL133–UL138* locus genes have important functions for replication and latency in hematopoietic cells, characterization in fibroblasts is important in defining the biology of these genes in HCMV infection and providing critical context for interpreting the functions and phenotypes of these genes apparent in hematopoietic cells. Fibroblasts were infected with *UL136*$_{\text{myc}}$, *UL136*$_{myc}$*ΔK→R*, *ΔUL135*$_{STOP}$*/UL136*$_{myc}$, or *ΔUL135*$_{STOP}$*/UL136*$_{myc}$*ΔK→R* at an MOI of 1 and viral protein accumulation was analyzed over a time course (Fig. 2A). As expected, UL135 protein was not detected in *ΔUL135*$_{STOP}$*/UL136*$_{myc}$ and *ΔUL135*$_{STOP}$*/UL136*$_{myc}$*ΔK→R* infections. Further, as previously reported, at a high MOI, proteins representative immediate early, early, and late (IE1/2, UL44, pp28, and pp150, respectively) viral gene expression follows the standard gene expression cascade in the absence of *UL135* (40). Stabilizing UL136p33 (*UL136*$_{\text{myc}}$*ΔK→R*) resulted in increased p33 protein levels, but decreased levels of middle *UL136* isoforms, particularly p25, relative to *UL136*$_{\text{myc}}$ infection (Fig. 2A and B). Further, stabilizing UL136p33 had little to no effect on early or late protein expression, represented by UL44 and pp150, respectively, relative to *UL136*$_{\text{myc}}$ infection (Fig. 2A and B). We detect no significant differences in IE or early gene expression between the mutant viruses. Although, as previously reported (40), viruses lacking *UL135* may produce modestly diminished levels of IE and early proteins in infection. Levels of the pp150 late protein were diminished in viruses lacking *UL135* and this was not rescued by the stabilization of UL136p33. With respect to the *UL136* isoforms, UL136p33 levels were elevated in *UL136*$_{\text{myc}}$*ΔK→R* infection, but only when *UL135* was present (Fig. 2A and C). We previously described the diminished accumulation of middle *UL136* isoforms during infection with *UL136*$_{myc}$*ΔK→R* (45). These results suggest that *UL135* is necessary for maximal accumulation of UL136p33 at late times, while increased expression of UL136p33 diminishes middle *UL136* isoform accumulation, some of which are pro-latency (43, 44).

Stabilization of UL136p33 does not rescue viral yields associated with disruption of *UL135* in productive infection

We previously have shown that disruption of *UL136p33* alone or stabilization of UL136p33 does not affect virus yields resulting from a productive infection in fibroblasts (43, 45). Further, we have previously reported that disruption of *UL135* results in a modest viral yield reduction in fibroblasts (40). To determine if stabilizing UL136p33 could rescue viral replication of Δ*UL135*$_{\text{STOP}}$, we performed a multi-step growth curve (MOI 0.02) in fibroblasts infected with *UL136*$_{\text{myc}}$, *UL136*$_{myc}$*ΔK→R*, *ΔUL135*$_{STOP}$*/UL136*$_{myc}$, or *ΔUL135*$_{STOP}$*/UL136*$_{myc}$*ΔK→R* recombinant viruses (Fig. 3A). While *UL136*$_{myc}$*ΔK→R* replicates with similar titers and yields as the parental virus, stabilization of UL136p33 did not compensate for the disruption of *UL135*; *ΔUL135*$_{STOP}$*/UL136*$_{myc}$*ΔK→R* replicated with similar kinetics and yields as *ΔUL135*$_{STOP}$*/UL136*$_{myc}$.

We also analyzed viral genomes amplified in cells infected with WT *UL136*$_{\text{myc}}$, *UL136*$_{myc}$*ΔK→R*, *ΔUL135*$_{STOP}$*/UL136*$_{myc}$, or *ΔUL135* $_{STOP}$*/UL136*$_{myc}$*ΔK→R* recombinant viruses at an MOI of 1 (Fig. 3B). Total viral genomes were quantified using real-time quantitative polymerase chain reaction (qPCR) with primers specific to sequences encoding the β2.7 region of the genome (46) at 6 and 72 hours post-infection (hpi). Viral genomes were amplified to similar levels in each infection, indicating that viral genome synthesis is not impacted by the loss of UL135 or the stabilization of UL136p33. The replication defect observed for Δ*UL135*$_{\text{STOP}}$ infection in fibroblasts is due to late-phase defects that were not rescued by the stabilization of UL136p33.

Increased UL136p33 concentration does not enhance viral gene expression separate from viral DNA synthesis

Maximal expression of *UL136* requires viral DNA synthesis (39, 40, 43). To examine the relationship between *UL136* and viral gene expression around viral DNA synthesis, we

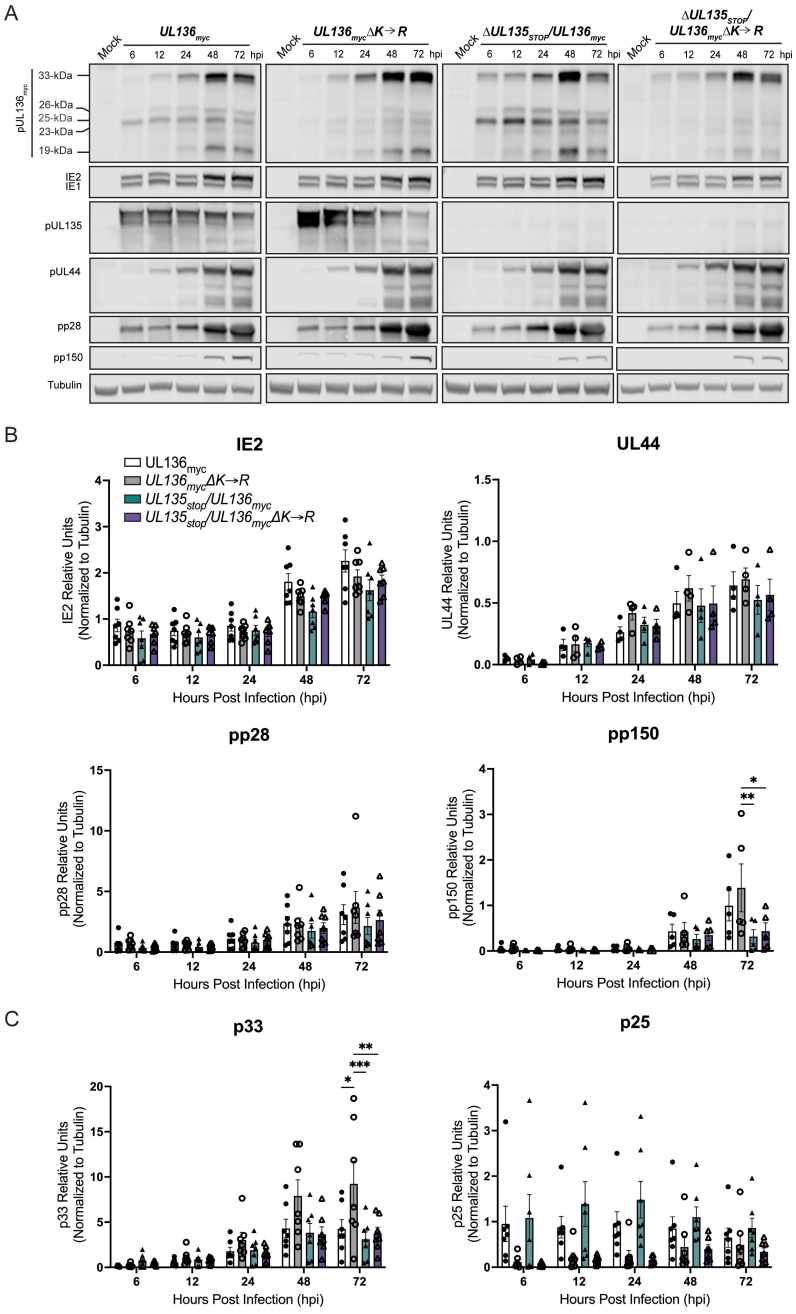

FIG 2 Stabilizing UL136p33 modestly alters viral gene expression in a productive infection. (A) MRC-5 lung fibroblast cells were infected with *UL136*$_{myc}$, *UL136*$_{myc}$*ΔK→R*, *ΔUL135*$_{STOP}$*/UL136*$_{myc}$, or *ΔUL135*$_{STOP}$*/UL136*$_{myc}$*ΔK→R* recombinant viruses at MOI of 1. Lysates were collected over a time course of infection and immunoblotted using antibodies specific to the myc epitope tag (*UL136* isoforms), *UL135* (*UL135* isoforms), *UL44*, IE1&2 (clone 3H4), pp28, and pp150. Tubulin was used as a loading control. Representative blots are shown. (B and C) Protein levels quantified over multiple independent experiments using Image Studio Lite quantification software. All protein bands are normalized to tubulin. Bars represent the averages of at least three independent experiments with standard deviation shown. Significance is calculated using a two-way ANOVA with Tukey's multiple comparison tests. **P* < 0.01; ***P* < 0.001; ****P* < 0.0001.

analyzed the accumulation of viral proteins in fibroblasts infected with *UL136*$_{myc}$ or *UL136*$_{myc}$*ΔK→R* and treated with phosphonoacetic acid (PAA) to inhibit HCMV genome

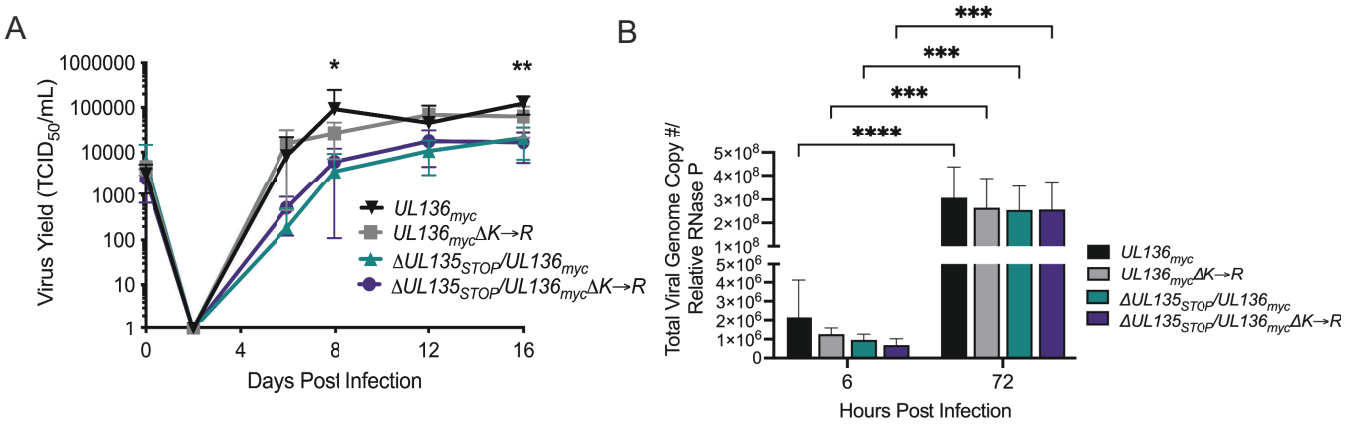

FIG 3 Stabilization of UL136p33 does not rescue viral yields associated with disruption of *UL135* in productive infection. (A) Primary MRC-5 cells were infected with WT $UL136_{myc}$, $UL136_{myc}\Delta K{\rightarrow}R$, $\Delta UL135_{STOP}/UL136_{myc}$, or $\Delta UL135_{STOP}/UL136_{myc}\Delta K{\rightarrow}R$ recombinant viruses, and a multistep (MOI of 0.02) growth curve was performed. Cells and culture supernatant were collected at the indicated time points, and virus titers were measured by $TCID_{50}$. Data points represent the averages from three independent experiments and error bars represent standard deviations. A two-way ANOVA with Tukey's multiple comparison tests were performed to determine statistical significance for each mutant infection relative to the WT $UL136_{myc}$ infection. $^{*}P < 0.05$ for WT $UL136_{myc}$ compared to $\Delta UL135_{STOP}/UL136_{myc}$ and $\Delta UL135_{STOP}/UL136_{myc}\Delta K{\rightarrow}R$ at 8 dpi and $^{**}P < 0.01$ for WT $UL136_{myc}$ compared to $\Delta UL135_{STOP}/UL136_{myc}$ and $\Delta UL135_{STOP}/UL136_{myc}\Delta K{\rightarrow}R$ at16 dpi. (B) Total DNA was isolated from primary MRC-5 cells infected at an MOI of 1 with WT $UL136_{myc}$, $UL136_{myc}\Delta K{\rightarrow}R$, $\Delta UL135_{STOP}/UL136_{myc}$, or $\Delta UL135_{STOP}/UL136_{myc}\Delta K{\rightarrow}R$ recombinant viruses at 6 and 72 hpi. The total number of viral genomes were quantified using qPCR with primers to β2.7kb relative to the cellular RNaseP gene. The viral genomes present in the cell at 6 hpi represent the input genome copy number. Averages of duplicate measurements from three independent experiments with standard deviation bars are shown for each virus at each time point. A two-way ANOVA with Tukey's multiple comparison tests were performed to determine statistical significance values for each mutant infection relative to its 6 hpi time point (***, $P < 0.001$ and ****, $P < 0.0001$).

synthesis or a vehicle control (Fig. 4A). As previously shown, PAA treatment diminishes the accumulation of *UL136* isoforms (43) and the canonical late protein, pp28, as well as amplification of IE2 at 48–72 hpi (43, 47, 48). While $UL136_{myc}\Delta K{\rightarrow}R$ increased levels of UL136p33, late-phase UL136p33 accumulation (48–72 hpi) is limited by PAA relative to the vehicle control (Fig. 4A). Quantification of UL136p33, UL135, IE2 and pp28 protein levels is shown in Fig. 4B. Stabilization of UL136p33 did not rescue late-phase IE2 or pp28 gene expression in infected cells where viral genome synthesis and entry into late phase was blocked by PAA (Fig. 4B). Further, stabilization of UL136p33 does not fully compensate for the onset of viral genome amplification and late-phase events in driving maximal UL136p33 accumulation.

Stabilizing UL136p33 does not direct middle *UL136* isoforms for proteasomal degradation

We have previously shown that UL136p33 is targeted for rapid proteasomal turnover by a host E3 ubiquitin ligase, IDOL (45). We next wanted to ask if the loss of middle *UL136* isoforms when UL136p33 is stabilized (Fig. 2) is due to proteasomal degradation. To investigate this, we infected cells with either $UL136_{myc}$ or $UL136_{myc}\Delta K{\rightarrow}R$ and treated cells with MG132 or vehicle 6 h prior to collecting lysates at 24 hpi (Fig. 5A). All UL136 isoforms are quantified over multiple independent replicates in Fig. 5B. As observed earlier, UL136p33 levels increased with MG132 treatment (45). Somewhat surprisingly, proteasomal inhibition also increased levels of $UL136_{myc}\Delta K{\rightarrow}R$, indicating that in addition to IDOL-dependent targeting to the proteasome, *UL136* may also be targeted

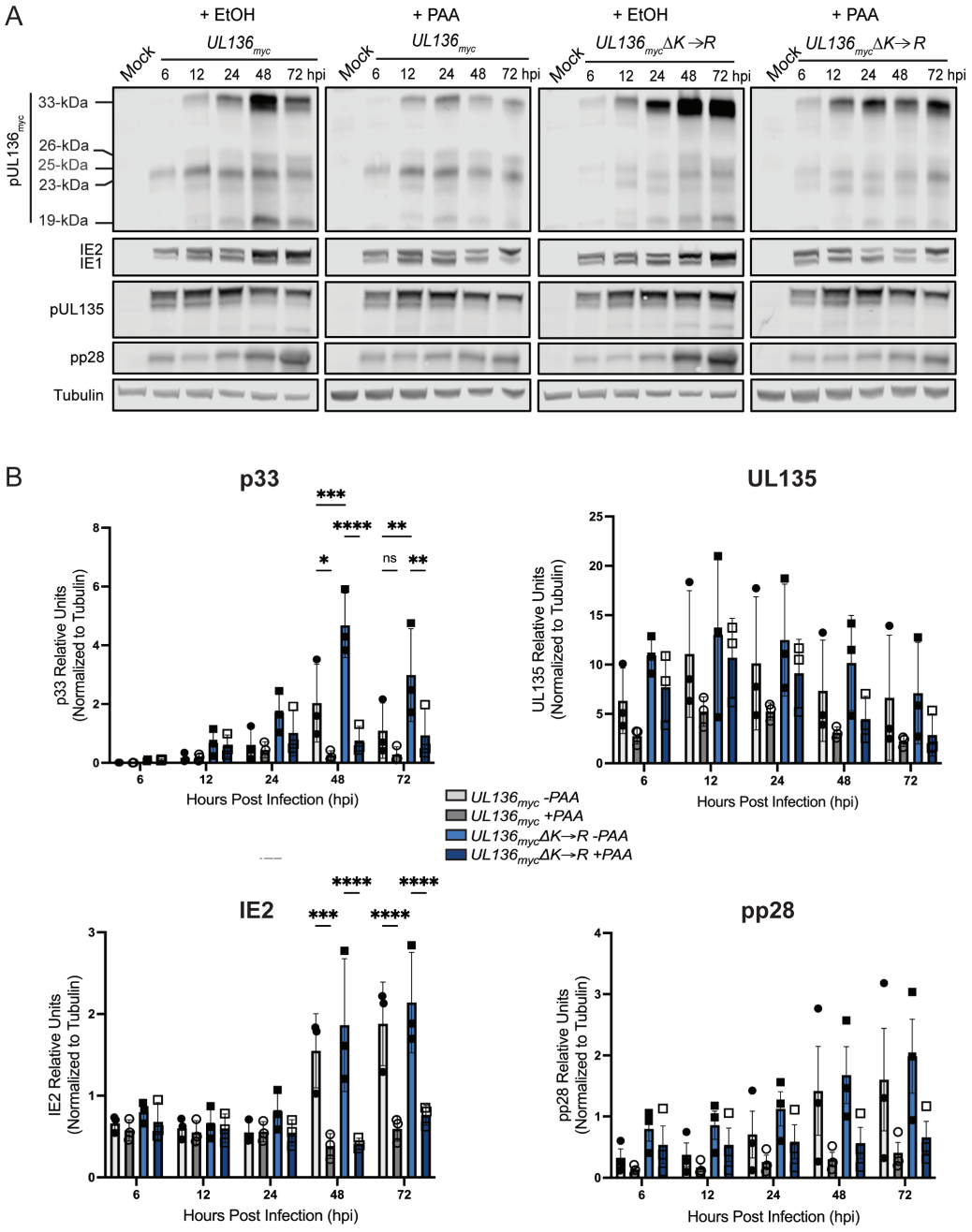

FIG 4 Increased UL136p33 concentration does not enhance viral gene expression separate from viral DNA synthesis. (A) MRC-5 cells were infected with WT *UL136*$_{myc}$ or *UL136*$_{myc}$*ΔK→R*, at an MOI of 1 and treated with PAA (50 µg/mL) or ethanol as the vehicle control at the time of infection. The drug was refreshed at 24 and 48 hpi to account for decay. Lysates were collected and immunoblotted at the indicated time points for viral proteins using antibodies described in Table 1. The tubulin antibody was used as a loading control. Representative blots are shown. (B) Multiple independent experiments were quantified. Data points represent the averages from three independent experiments, and error bars represent standard deviations. A two-way ANOVA with Tukey's multiple comparison tests were performed to determine the statistical significance values for each infection relative to PAA treatment at each time point. *, $P < 0.05$; **, $P < 0.01$; ***, $P < 0.001$; ****, $P < 0.0001$.

for ubiquitin-independent, proteasome-dependent turnover. Ubiquitin-independent, proteasome-dependent turnover has been reported as a mechanism by which the HCMV tegument protein pp71 targets host factors (49, 50), including the retinoblastoma protein and Daxx for destruction, as well as other viral or cellular oncoproteins (51–53). More work is required to fully investigate this possibility.

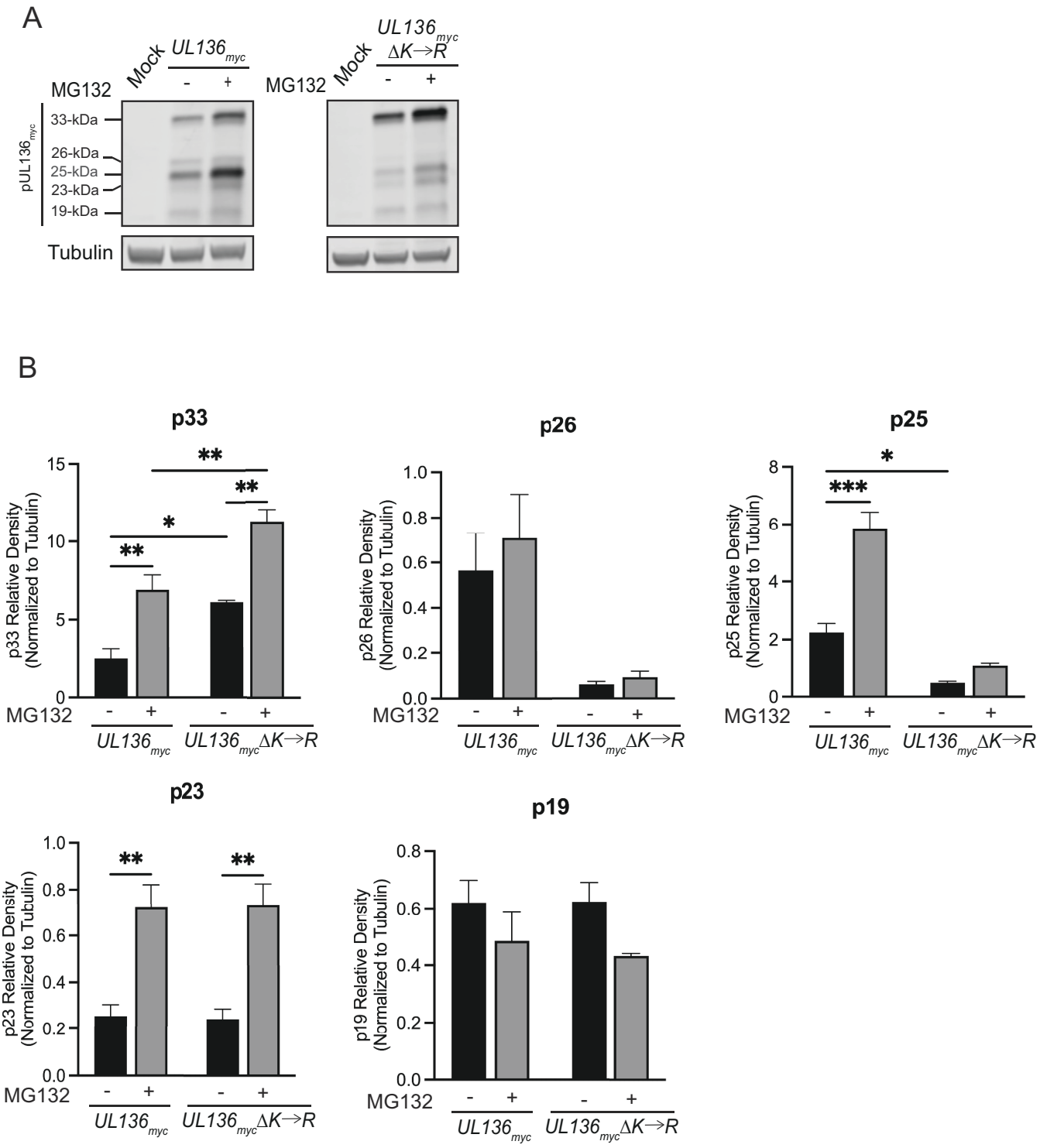

FIG 5 Stabilizing UL136p33 does not direct the middle isoforms of *UL136* for proteasomal degradation. MRC-5 fibroblasts were infected with either $UL136_{myc}$ or $UL136_{myc}\Delta K{\rightarrow}R$. 6 h prior to lysate collection, infected cells were treated with 20 μM MG132 to inhibit the proteasome or vehicle control. Lysates were collected at 24 hpi and immunoblotted for myc to detect protein isoforms and tubulin (as a loading control) with antibodies described in Table 2. Three independent biological replicates were used to calculate statistical significance. Statistical significance was calculated through a two-way ANOVA with Tukey's multiple comparison tests for each isoform as follows. *, $P < 0.05$; **, $P < 0.01$; ***, $P < 0.001$; ****, $P < 0.0001$.

There are four lysine residues in UL136p33 (K4, K20, K25, and K113) and only K113 is shared by the UL136 isoforms smaller than p33. Like UL136p33, p25 and p23 are also rescued by MG132 treatment, indicating that they are targeted to the proteosome. MG132 has no effect on p25 levels in the K→R mutant virus, suggesting that ubiquitination of K113 is required for its turnover. However, we have shown that IDOL does not target p25 (45) and so may be targeted by a distinct E3 ubiquitin ligase. UL136p23 expressed from the K→R mutant virus is rescued by MG132-treatment, indicating that it may be targeted for proteasome-dependent degradation, independently of ubiquitination at K113. UL136p26 levels were not affected by MG132, although UL136p26 levels were reduced in the K→R mutant virus infection, suggesting that this protein is not targeted for proteasomal degradation but that the stabilization of UL136p33 negatively affects the expression of p26. Lastly, UL136p19 was not affected by K→R substitution or by proteasomal inhibition, suggesting that UL136p19 is not regulated by the proteasome or UL136p33. Taken together, these results indicate that UL136p33 negatively impacts the expression of p26 and p25 through non-proteasomal degradation. Heightened UL136p33 levels likely downregulate transcription of smaller isoforms. However, differential transcriptional regulation of the UL136 isoforms is difficult to assess since UL136 isoforms are expressed from overlapping transcripts generated by alternative transcriptional start sites (43).

Stabilizing UL136p33 rescues viral replication in the absence of *UL135* in CD34$^+$ HPCs

Both *UL135* and *UL136p33* are required for reactivation from latency (40, 44). Further, stabilization of UL136p33 results in virus that produces increased frequencies of infectious centers in CD34$^+$ HPCs in the absence of a reactivation stimulus (45). This result indicates that the instability of UL136p33 is important for the establishment of latency. We next wanted to determine if stabilizing UL136p33 could compensate for a loss of *UL135* in driving reactivation from latency in CD34$^+$ HPCs. We infected CD34$^+$ HPCs with WT $UL136_{myc}$, $UL136_{myc}\Delta33kDa$ (*TB40/E* $UL136_{myc}$ containing a stop codon disruption of the UL136p33 isoform) (44), $UL136_{myc}\Delta K{\rightarrow}R$, and $\Delta UL135_{STOP}/UL136_{myc}\Delta K{\rightarrow}R$ recombinant viruses. Infected HPCs (CD34$^+$/GFP$^+$) were purified by FACS and seeded into long-term bone marrow culture over a stromal cell support. At 10 dpi, the infected cell culture was split. Half the culture (live cells) was seeded by limiting dilution onto permissive fibroblast monolayers in a cytokine-rich medium to stimulate differentiation and reactivation (Reactivation). The other half of the culture was lysed and seeded in parallel on top permissive fibroblast monolayers by limiting dilution to determine infectious centers present prior to reactivation (Pre-Reactivation control) (54) (Fig. 6A). While we were unable to produce high enough titer stocks of the $\Delta UL135_{STOP}/UL136_{myc}$ virus sufficient for infection of CD34$^+$ HPCs for all replicates, we have previously shown that $\Delta UL135_{STOP}$ viruses fail to reactivate, similarly to the $UL136_{myc}\Delta33kDa$ infection (40, 55). As previously reported, the $UL136_{myc}\Delta K{\rightarrow}R$ infection resulted in a virus that replicated in CD34$^+$ HPCs in the absence of a replication stimulus (45), indicating an inability to establish latency. Intriguingly, $\Delta UL135_{STOP}/UL136_{myc}\Delta K{\rightarrow}R$ infection resulted in a virus that was equally as replicative as $UL136_{myc}\Delta K{\rightarrow}R$. These data indicate that when UL136p33 is stabilized, the loss of UL135 has little or no consequence for replication in hematopoietic cells. We also analyzed viral genome copy number at 10 dpi in two independent experiments using two independent donors (Fig. 6B). Consistent with the infectious centers measurements, viral genome levels were equivalent to or greater in the $\Delta UL135_{STOP}/UL136_{myc}\Delta K{\rightarrow}R$ infection relative to $UL136_{myc}\Delta K{\rightarrow}R$ infection. Taken together, these findings suggest that stabilization of UL136p33 can rescue the defect in replication associated with the loss of *UL135* in CD34$^+$ HPCs and suggest cell type-dependent functions or mechanisms for the *UL133/8* locus genes.

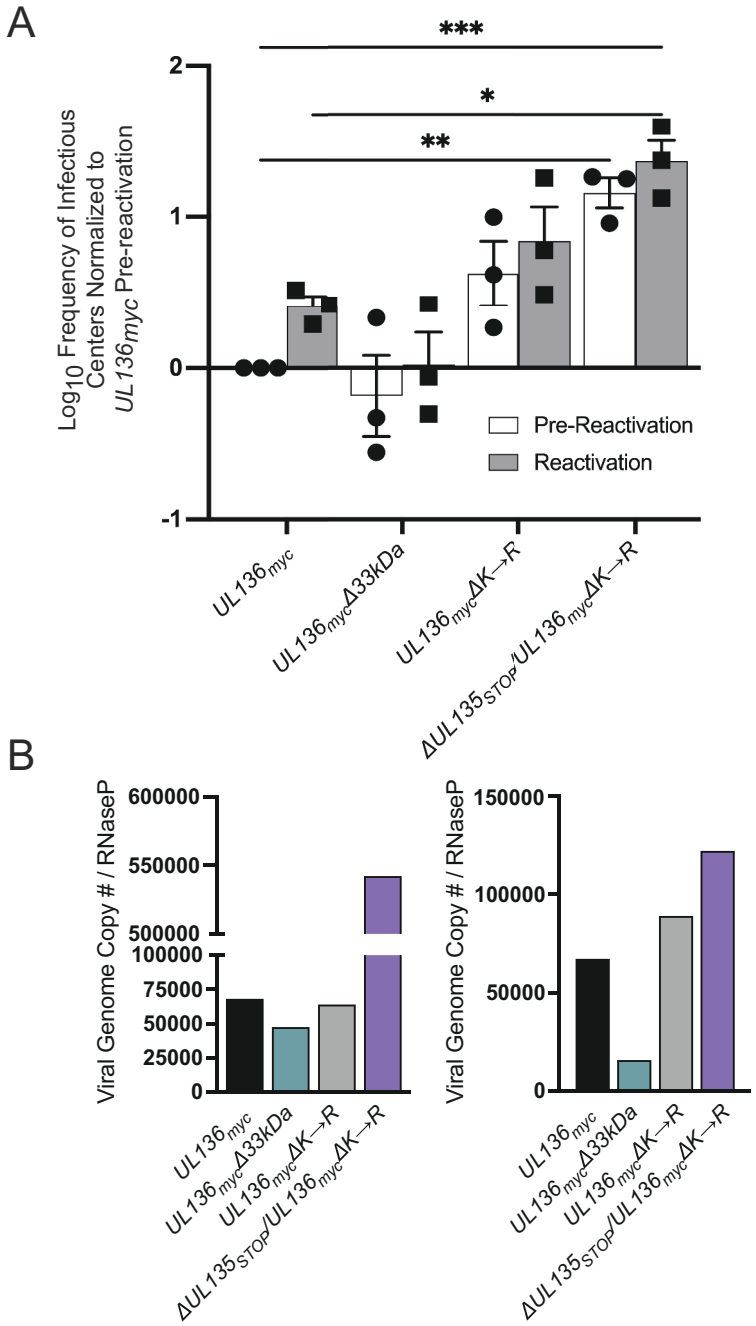

FIG 6 Stabilizing UL136p33 rescues viral replication in the absence of UL135 in CD34$^+$ HPCs. (A) CD34$^+$ HPCs were infected with WT *UL136$_{myc}$*, *UL136$_{myc}$Δ33kDa*, *UL136$_{myc}$ΔK→R*, and *ΔUL135$_{STOP}$/UL136$_{myc}$ΔK→R* at an MOI of 2. At 24 hpi, CD34$^+$/GFP$^+$ (infected cells) were sorted and seeded into long-term bone marrow culture. After 10 days in culture, parallel populations of either mechanically lysed cells or live cells were plated onto fibroblast monolayers in cytokine-rich media. 14 days later, GFP$^+$ wells were scored, and the frequency of infectious centers was determined by extreme limiting dilution analysis. The mechanically lysed population defines the quantity of virus present prior to reactivation (pre-reactivation; white bar). The live-cell population defines the quantity of virus present after reactivation (reactivation; gray bar). The frequency was normalized to WT *UL136$_{myc}$* pre-reactivation, and the average of three independent experiments is shown. Statistical significance was calculated using a two-way ANOVA with Tukey's multiple comparison tests. *, $P < 0.05$; **, $P < 0.01$; ***, $P < 0.001$). (B) Total

FIG 6 (Continued)

DNA was isolated from CD34$^+$ HPCs infected with WT *UL136*$_{myc}$, *UL136*$_{myc}$*Δ33kDa, UL136*$_{myc}$*ΔK→R*, and *ΔUL135*$_{STOP}$*/UL136*$_{myc}$*ΔK→R* at an MOI of 2 at 10 dpi. The number of viral genomes relative to the level of RNaseP expression was quantified by qPCR using β2.7kb RNA gene- and RNaseP-specific primers. Two biological replicates from two independent cell donors are shown.

Stabilizing UL136p33 compensates for the loss of *UL135* for viral replication in huNSG mice

We next wanted to analyze the activity of these recombinant viruses in NOD-*scid* IL2Rγ$_c^{null}$ (huNSG) mice. We have previously demonstrated that UL136p33 is necessary for reactivation of HCMV post-G-CSF stimulation in huNSG mice engrafted with CD34$^+$ HPCs (44). While the huNSG mouse model has typically recapitulated results from our *in vitro* CD34$^+$ HPC experimental latency model, the one notable exception is for the *UL136*$_{myc}$*Δ25* kDa virus, which fails to reactivate in huNSG mice, but is more replicative in CD34$^+$ HPCs infected *in vitro* (44). huNSG mice were sublethally irradiated and engrafted with human CD34$^+$ HPCs. After CD34$^+$ engraftment, mice were injected with human fibroblasts infected with WT *UL136*$_{myc}$, *UL136*$_{myc}$*Δ33kDa, UL136*$_{myc}$*ΔK→R*, and *ΔUL135*$_{STOP}$*/UL136*$_{myc}$*ΔK→R* recombinant viruses. At 4 wk post-infection, five mice from each group of 10 were treated with G-CSF and AMD-3100 to induce stem cell mobilization and HCMV reactivation. At 1 wk post-mobilization, viral genome load was assessed in spleen and liver tissues from treated and untreated mouse groups to evaluate amplification of viral genomes and dissemination of infected cells to organs, as described previously (44).

As previously demonstrated, G-CSF mobilization of *UL136*$_{myc}$-infected humanized mice resulted in increased viral genomes detected in the spleen and liver relative to unmobilized mice, consistent with reactivation of virus replication (Fig. 7). By contrast, *UL136*$_{myc}$Δ33 kDa failed to reactivate and similar levels of genomes were measured in G-CSF/AMD-3100-treated as compared to untreated huNSG mice infected with either *UL136*$_{myc}$ or *UL136*$_{myc}$*Δ33kDa*. The viral genome copy number in the unmobilized and mobilized mice infected with *UL136*$_{myc}$*ΔK→R* was equivalent to the G-CSF/AMD-3100-mobilized *UL136*$_{myc}$ infection, indicating a failure to establish latency (replication in the absence of a stimulus). This phenotype recapitulates the *UL136*$_{myc}$*ΔK→R* phenotype in CD34$^+$ HPCs infected *in vitro* (Fig. 6). Strikingly, the *ΔUL135*$_{STOP}$*/UL136*$_{myc}$*ΔK→R* virus also recapitulated our *in vitro* studies with increased viral genome levels in the spleen and liver regardless of G-CSF/AMD-3100 treatment compared to mice infected with *UL136*$_{myc}$*ΔK→R*. Taken together, these results support an epistatic relationship between *UL135* and *UL136*, whereby stabilization of UL136p33 compensates for the loss of *UL135* in replication following a reactivation stimulus. Further, these data suggest a restrictive or deleterious consequence of *UL135* function in reactivation and replication and that these defects can be overcome by robust expression of UL136p33.

DISCUSSION

Viruses use complex gene-regulatory networks to coordinate major infection checkpoints. To direct the transition from latency to reactivation, herpesviruses must sense and respond to environmental cues and integrate multiple cellular states to exit the latent state for replication. HCMV has a large coding capacity of more than 170 genes for regulating infection in multiple cell types with the possibility of a much-expanded array of open reading frames (56). Many genes encode multiple proteins (referred to as isoforms), as is the case for UL136, UL44, UL99, and UL112-113, through alternative transcriptional and/or translational start sites within a single gene (34, 43, 57–61). Other herpesviruses, such as Kaposi's sarcoma-associated herpesvirus (KSHV) and herpes simplex type-1 (HSV-1), also have genes that encode for multiple protein isoforms with differential spatiotemporal expression, for example, ORF50 and UL12, respectively (62,

(Continued on next page)

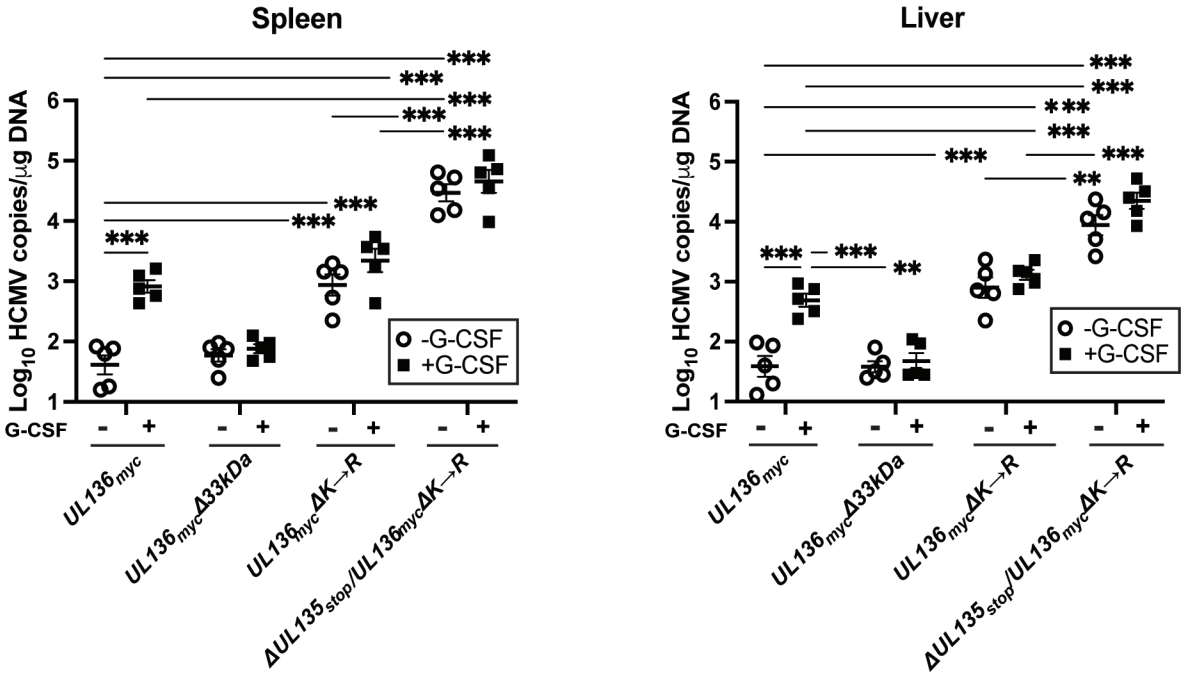

FIG 7 Stabilizing UL136p33 compensates for a loss of *UL135* for viral replication in huNSG mice. Humanized NSG mice were injected with fibroblasts infected with either HCMV WT $UL136_{myc}$, $UL136_{myc}\Delta 33kDa$, $UL136_{myc}\Delta K{\rightarrow}R$, and $\Delta UL135_{STOP}/UL136_{myc}\Delta K{\rightarrow}R$ ($n = 10$ per group). At 4 wk post-infection, half of the mice were treated with G-CSF and AMD-3100 to induce cellular mobilization and promote HCMV reactivation. Control mice were left untreated. At 1 wk post-mobilization, mice were euthanized, and tissues were collected. Total DNA was extracted using DNAzol, and HCMV viral load was determined by qPCR on 1 µg of total DNA prepared from spleen or liver tissue. Error bars represent standard error of the mean between average DNA copies from two or four tissue sections, respectively, for individual animals. All samples were compared by a two-way ANOVA with Tukey's multiple comparison tests within experimental groups (nonmobilized [-G-CSF] versus mobilized [+G-CSF] for each virus and between all virus groups for both nonmobilized and mobilized conditions). Statistical significance where **, $P < 0.01$ and ***, $P < 0.001$.

63). While the full potential of protein isoforms encoded by herpesviruses remains to be defined, genes encoding multiple proteins allow for coordinated regulation of effectors to dictate infection outcomes. Protein isoforms encoded from a single gene may have synergistic or opposing roles (e.g., dominant negative) in dictating patterns of infection in a context-dependent manner (4). Further, epistatic interactions of viral genes in the same locus (or gene circuit) add to the complexity of HCMV biology. This work investigates the role of *UL136*, specifically the instability of the UL136p33 isoform, and its epistatic relationship with UL135 in driving replication. This question is significant to understanding the complex, context-dependent interactions between virus–virus and virus–host factors that influence the "decision" to enter and maintain latency or to reactivate from latency.

Both UL135 and UL136p33 are important for reactivation from latency (40, 44). UL135-mutant viruses exhibit a modest defect for replication and production of progeny virus in fibroblasts (34, 40), whereas disruption or stabilization of UL136p33 had no impact on replication in fibroblasts (43, 45). *UL135* and *UL136* are also important for replication in endothelial cells (64). While stabilizing UL136p33 did not compensate for the loss of *UL135* in late gene expression or virus yields during infection in fibroblasts (Fig. 2 and 3), stabilization of UL136p33 strikingly compensated for the loss of *UL135* in hematopoietic cells infected *in vitro* and in humanized mice, resulting in increased virus replication in HPCs in the absence of a stimulus for reactivation (Fig. 6 and 7). This indicates distinct cell type-dependent roles for UL135 and UL136p33 for replication. These findings suggest that while UL135 is important to the initiation of or commitment to replication, accumulation of UL136p33 represents a subsequent threshold for replication. Once UL136p33 accumulation is ensured, in this case experimentally by lysine to arginine substitution, the additional loss of UL135 does not confer

a disadvantage for replication and reactivation in experimental HPC models of latency. A limitation in the interpretation of these findings is our inability to acquire enough cells infected with the UL135-mutant virus expressing UL136myc for latency assays. UL135-mutant viruses are very difficult to reconstitute from transfection of infectious BAC clones and exhibit a defect for reactivation, although virus stocks once achieved have only a modest defect for replication in fibroblasts. Further work is required to determine phenotypes associated with these viruses during infection in endothelial or epithelial cells. It is possible that stabilization of UL136p33 may complement the replication defect associated with loss of UL135 during infection in endothelial cells.

In collaboration with the Kamil lab, we previously defined an epistatic relationship between *UL135* and *UL97* in promoting late-phase viral gene expression, viral DNA synthesis, and viral replication in a productive infection (41). In these studies, UL97, the only HCMV-encoded kinase, was remarkably dispensable for replication in the AD169 laboratory-adapted strain (42). However, the loss of UL97 conferred defects in replication in fibroblasts in low-passage strains containing the UL*b*′ region of the viral genome that is lost from laboratory-adapted strains. Analysis of recombinant viruses containing mutations in the *UL133–UL138* locus genes identified *UL135* as the gene that conferred a requirement for UL97 for virus infection. In other words, UL97 compensated for deleterious effects on infection due to the action *UL135*, such inhibition of UL97 only conferred defects on virus replication when UL135 was expressed (41). Similarly, the recombinant $UL135_{STOP}/UL136_{myc}\Delta K{\rightarrow}R$ virus replicates efficiently without a reactivation stimulus and to enhanced levels compared to the parental virus or a virus disrupted for expression of UL136p33, particularly in the humanized mouse model (Fig. 6 and 7). Taken together with the *UL97/UL135* relationship, the present study suggests that *UL135* functions, while important for reactivation, pose deleterious consequences for virus replication and other viral genes function to mitigate those effects. The requirement for *UL135* in replication in hematopoietic cells was dispensable when UL136p33 was stabilized, suggesting that *UL135* function is important in stimulating activities in infection that result in the accumulation of UL136p33. The temporal expression and relative accumulation of *UL135* and *UL136* gene products to required thresholds are undoubtedly important for the progression to successful reactivation.

While *UL135* is expressed with early kinetics, *UL136* and *UL97* are expressed with early/late or leaky late kinetics and their maximal accumulation requires viral DNA synthesis and entry into late phase (43, 65). These kinetics and the instability of UL136p33 suggest a model whereby latency depends both on *UL138* and the instability UL136p33 (Fig. 8). Reactivation from latency, by contrast, depends on the expression of *UL135*, which functions, at least in part, to overcome the suppressive effects of *UL138* (40, 66) and to drive infection for the eventual accumulation of UL136p33. At the same time, *UL97* expression may compensate for deleterious effects of *UL135* (41). As UL136p33 accumulation is further fortified by the initiation of viral DNA synthesis (Fig. 4), this indicates a second checkpoint (following *UL135* expression) in the commitment to reactivation and replication (Fig. 8). This model suggests a stepwise progression toward reactivation where thresholds must be met to pass checkpoints that would otherwise block reactivation and maintain latency. Much remains to be understood about the UL135-UL136 interaction and the mechanisms through which they function to control latency-reactivatation decisons. While UL135 and UL136 may physically interact, it is as likely that they co-regulate cellular pathways.

Cellular factors are critical to HCMV latency through, at least in part, their impact on viral gene expression and proteins. We have previously shown that UL138 expression is driven by binding of the host EGR-1 transcription factor to sites just upstream of UL136 (67). As EGR-1 is highly expressed in HPCs, these cells are primed to express UL138, and the ratio of transcripts encoding UL138 to those encoding UL135 is high. We have also shown that UL136p33 is maintained at low levels by the host E3 ubiquitin ligase, IDOL, which is also highly expressed in undifferentiated hematopoietic cells (45). Both EGR-1

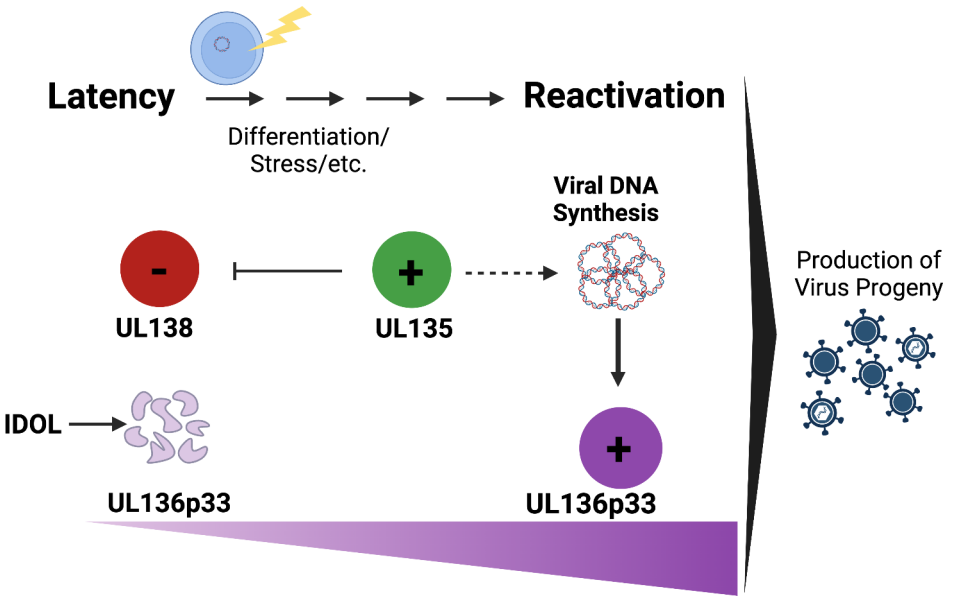

FIG 8 Model for *UL135* and UL136p33 epistasis for coordinating reactivation of HCMV. We have previously shown that viral factors, such as UL138, function in a pro-latency manner in the establishment of latency, whereas UL135 and UL136p33 function in a pro-reactivation manner. We have further demonstrated that the instability of UL136p33, driven by the IDOL ubiquitin E3 ligase, is also important for the establishment of latency. Reactivation cues stimulate increased expression of UL135 relative to UL138 and increased accumulation of UL136p33 through two mechanisms: (i) the loss of IDOL and (ii) increased UL136p33 synthesis following commitment to viral DNA synthesis. Because ensuring the accumulation of UL136p33 through its stabilization precludes the need for UL135 for replication in HPCs, we propose the existence of checkpoints in the decision to reactivate where UL135 initiates reactivation and subsequent accumulation of UL136p33 is required to meet a threshold in the commitment to reactivation. Created with BioRender.com.

and IDOL expression are sharply downregulated by differentiation (45, 67), a well-appreciated trigger of HCMV reactivation (4, 68). Therefore, differentiation is expected to increase the ratio of UL135 transcripts relative to UL138 transcripts (67) and increase the accumulation of UL136p33, which is further amplified by the onset of viral DNA synthesis and entry into late phase. Additional work is required to understand how UL135 functions to promote the progression of infection toward replication and the accumulation of UL136p33. UL135 is well-appreciated for its role in modulating host signaling and cytoskeletal organization, and these roles could impact the expression of *UL136* indirectly (55, 66, 69).

Interactions (either physical or by differentially impacting the same processes in infection) between *UL136* isoforms or with other UL133/8 locus proteins represent important questions for further investigation. We have shown that while UL136p33 and p26 are important for reactivation, UL136p23/p19 are suppressive to replication for latency (44). The antagonistic or synergistic roles of the UL136 protein isoforms may allow the virus to navigate the commitment to reactivation or the maintenance of latency. The decision to maintain latency or reactivate at the point of viral DNA synthesis may depend on competition between or the differential accumulation of UL136 isoforms (44).

We have demonstrated here that stabilization of UL136p33 leads to a reduction in the protein levels of the middle UL136 isoforms (Fig. 2, 4, and 5), which may aid in allowing HCMV to commit to reactivation and replication. It will be important to define both transcriptional and posttranslational mechanisms regulating UL136 isoform accumulation. UL136 isoforms are synthesized from unique transcripts derived from alternative transcriptional start sites and may be regulated in a context-dependent manner (43). The promoter elements driving UL136 isoform expression have not been characterized. We have shown previously that HCMV reactivation from latency stimulates major immediate

early gene expression from alternative promoter sequences embedded within intron A of the MIE transcriptional unit, while the MIEP apparently remains silent (47). In addition, KSHV *Orf50* encodes four different protein isoforms of the replication and transcription activator protein, RTA, that temporally regulate each other's expression for driving the viral gene expression cascade post-reactivation (62). This study demonstrated specifically that induction of the upstream *Orf50* N5 promoter that produces RTA isoform four suppresses expression of RTA isoform one through transcriptional interference. Further work is required to define the promoters and transcription factors governing UL136 isoform expression and their impact on one another. Beyond transcriptional regulation, some isoforms are targeted for proteasomal degradation (p33, p25, and p23), while others are not (p26 and p19). Of those targeted for proteasomal degradation, p23 appears to be targeted by ubiquitin-independent mechanisms since K→R substitution had no effect on its turnover. Finally, differential regulation of distinct UL136 protein isoforms may reflect their distinct subcellular localization (44).

This study highlights the complexity of the *UL133–UL138* gene network and its phenotypes depending on the context of infection. The ability of a virus to move between bistable infection states—latency or replication—requires that the virus can "sense" host cues, filter and utilize fluctuations ("noise") to respond appropriately to the host cues to regulate infection fate decisions. UL136p33 may function in an ultrasensitive manner to control the switch for reactivation upon differentiation of HPCs—rapid accumulation of UL136p33 to a threshold to tip the system to reactivation (70). Going forward, it will be important to define how expression from the *UL133–UL138* locus is regulated and if UL136 isoforms help the virus stabilize or filter noise to understand HCMV fate decisions.

MATERIALS AND METHODS

Cells

Human primary embryonic lung fibroblasts (MRC-5, purchased from ATCC; Manassas, VA) were cultured in Dulbecco's modified Eagle's medium (DMEM) and supplemented with 10% fetal bovine serum (FBS), 10 mM HEPES, 1 mM sodium pyruvate, 2 mM L-alanyl-glutamine, 0.1 mM nonessential amino acids, 100 U/mL penicillin, and 100 µg/mL streptomycin. The Institutional Review Board approved a protocol to obtain human cells from bone marrow transplant waste at the University Medical Center at the University of Arizona. Specimens were de-identified and provided as completely anonymous samples. $CD34^+$ HPCs were isolated and cultured as previously described (34, 54). Briefly, $CD34^+$ HPCs were isolated using the CD34 MicroBead Kit (MACS, Miltenyi Biotec, San Diego, CA). Pure populations of $CD34^+$ HPCs were subsequently cultured in MyeloCult H5100 (Stem Cell Technologies, Cambridge, MA) supplemented with hydrocortisone, 100 U/mL penicillin, and 100 µg/mL streptomycin and maintained in long-term co-culture with M2-10B4 and Sl/Sl murine stromal cell lines (kind gift from Stem Cell Technologies on behalf of D. Hogge, Terry Fox Laboratory, University of British Columbia, Vancouver, BC, Canada) (34, 54). All cells were maintained at 37°C with 5% CO_2.

Recombinant viruses

The TB40/E BAC was engineered to express the green fluorescent protein (GFP) driven by the SV40 early promoter located in the intergenic region in between US34 and TRS1 genes as a marker for infection (34, 71). All recombinant viruses were created using a two-step, positive/negative selection approach that leaves no trace of the recombination process (39, 72, 73). Three recombinant viruses used in this study were previously engineered—$UL136_{myc}$,$UL136_{myc}\Delta 33kDa$, and $UL136_{myc}\Delta K{\rightarrow}R$—as described previously (43, 45). Two new recombinant viruses were generated for this study—$\Delta UL135_{STOP}/UL136_{myc}$ (to detect the UL136 isoforms when *UL135* is disrupted) and $\Delta UL135_{STOP}/UL136_{myc}\Delta K{\rightarrow}R$ (where UL136p33 is stabilized when *UL135* is disrupted). We previously

TABLE 1 Primers used in this study for BAC recombineering

Primer name	Primer sequence
UL135 (bp854) Forward	5′-CGGAGCCGACCACGC TGCCTATCG-3′
UL138(bp 139) Reverse	5′-GCCAGCGGTAGCTCAAAAACATGCGC-3′

generated a *UL135*$_{stop}$ *UL136* <*GalK* > intermediate virus that serves as the base BAC for the two new recombinant viruses created in this study (64). The "*UL136*$_{myc}$" and "*UL136*$_{myc}$*ΔK→R*" sequence mutations were PCR amplified off of BACs previously made and characterized with these desired mutations using the following primers: UL138 (139 bp) Rev and UL135 (854 bp) Fwd (43, 45). The sequences for the primers used for this amplification are listed in Table 1. The PCR-amplified products were then recombined into the *UL135*$_{stop}$ *UL136* <*GalK* > BAC as described previously (43, 64). BAC integrity was tested by enzyme digest fragment analysis and sequencing of the *UL136* region using the same primers described in 1. All BAC genomes were maintained in SW102 *Escherichia coli* and viral stocks were propagated by transfecting 15–20 µg of each BAC genome, along with 2 µg of a plasmid encoding *UL82* (pp71) into 5×10^6 MRC-5 fibroblasts, allowed to propagate in MRC-5 fibroblasts and then subsequently purified and stored as previously described to generate the parent (P0) virus (39). To grow the next generation of each virus (P1), the infectious inoculum from the P0 virus was added to MRC-5 fibroblasts that were passaged into roller bottles and cultured for anywhere from 8 to 30 days depending on the recombinant virus being made. Viruses were subsequently purified and stored as previously described (39). Virus titers were determined by 50% tissue culture infectious dose ($TCID_{50}$) on MRC-5 fibroblasts.

Whole-genome next-generation sequencing and computational analysis

Seven recombinant HCMV BAC genome DNAs were extracted from SW102 *E. coli* propagating each HCMV genome using a BAC miniprep DNA isolation method. DNA was then sent to SeqCenter, LLC for short read Illumina whole-genome sequencing using an Illumina NextSeq 2000 (200 Mbp sequencing package—https://www.seqcenter.com/dna-sequencing/). Demultiplexing, quality control, and adapter trimming were performed with bcl-convert (v3.9.3). The single-nucleotide polymorphisms (SNPs) were identified using a python package called SNIPPY (https://github.com/tseemann/snippy, accessed June 23, 2022). Analysis is based on the BWA-mem/freebayes pipeline that identifies the mutations between a haploid reference genome and the next-generation sequence reads. The package was implemented with default parameters on the University of Arizona High Performance Computing (HPC) environment, dedicating 80 GB RAM for the job. SNIPPY was able to identify SNPs, multi-nucleotide polymorphisms (MNPs), complex mutations as well as indels.

Immunoblotting

Immunoblotting was performed as previously described (39, 43). Briefly, 50 µg of protein lysate were separated on 12% bis-tris gels by electrophoresis and transferred to 0.45 µm polyvinylidene difluoride (Immobilon-FL, Millipore) membranes. Proteins were detected using epitope- or protein-specific antibodies and fluorescently conjugated secondary antibodies using the Odyssey infrared imaging system (Li-Cor). All antibodies were used as listed in Table 2. Where indicated, cells were treated with 50–100µg of PAA, 1–50µM MG132, or vehicle control. We are grateful for the gift of antibodies from Drs. Thomas Shenk, William Britt, and John Purdy.

Viral growth curves

Quantification of infectious virus produced by fibroblasts was determined by infecting MRC-5s at an MOI of 0.02 and subsequently collecting cells and medium over a 16-day infection time course. Virus titers were determined by $TCID_{50}$ in MRC-5 fibroblasts.

TABLE 2 List of antibodies used in this study

Antigen	Antibody	Concentration	Animal	Source
myc epitope-M	9B11	1:1,000	Mouse	Cell Signaling
myc epitope-R	71D10	1:1,000	Rabbit	Cell Signaling
myc epitope-R		1:1,000	Rabbit	Proteintech
alpha-tubulin	DM1A	1:2,000	Mouse	Sigma
UL138		1:500	Rabbit	Open Biosystems
UL135		use at 2 ug/mL	Rabbit	Open Biosystems
IE1&2	3H4	1:250	Mouse	Gift, Dr. Thomas Shenk through John Purdy
pp150		1:15	Mouse	Gift from Dr. William Britt
pp28 (UL99)	10B4-29	1:50	Mouse	Gift, Dr. Thomas Shenk
UL44	10D8	1:12,000	Mouse	Virusys

Quantification of viral genomes in fibroblasts

Total DNA was isolated from ~6×10^5 to 7×10^5 MRC-5-infected fibroblasts using the Zymo Duet RNA/DNA isolation Kit (Zymo Research). Viral genomes were quantitated by quantitative PCR (qPCR) using the LightCycler 480 1X SYBR Green master mix (Roche) according to the manufacturer's instructions. Primers specific to the noncoding b2.7 RNA gene were used. To determine the number of viral genomes present, viral DNA copy numbers were quantified relative to a BAC standard curve normalized to a cellular housekeeping gene RNase *P* as previously described (47).

Infectious centers assay

$CD34^+$ HPCs, isolated from human cord blood, were used to assess latency and reactivation of HCMV *in vitro* as previously described (34, 54). Briefly, $CD34^+$ HPCs were infected at an MOI of 2 for 20 h after which a pure population (>97%) of infected (GFP^+) $CD34^+$ cells were isolated via FACS (FACSAria, BD Biosciences Immunocytometry Systems, San Jose, CA, USA) using a phycoerythrin-conjugated CD34-specific antibody (BD Biosciences) and propidium iodide to exclude dead cells. These cells were cultured in transwells above irradiated (4,000 rads, ^{137}Cs gammacell-40 irradiator type B, Atomic Energy of Canada LTD, Ottawa, Canada) M2-10B4 and SI/SI stromal cells for 10 days. The frequency of the production of infectious centers was measured using an extreme limiting dilution assay as described previously (34, 54). The frequency of infectious centers, based on the number of GFP^+ cells at 14 days post-plating, was calculated using ELDA, extreme limiting dilution analysis software (http://bioinf.wehi.edu.au/software/elda/) (74).

Engraftment and infection of huNSG mice

All animal studies were carried out in strict accordance with the recommendations of the American Association for Accreditation of Laboratory Animal Care (AAALAC). The protocol was approved by the Institutional Animal Care and Use Committee (protocol 0922) at the Vaccine and Gene Therapy Institute (OHSU). NOD-*scid* $IL2R\gamma_c^{null}$ mice were maintained at a pathogen-free facility at Oregon Health and Science University in accordance with procedures approved by the Institutional Animal Care and Use Committee. Both sexes of animals were used. Humanized mice were generated as previously described (44, 75). The animals (12–14 wk post-engraftment) were treated with 1 mL of 4% thioglycolate (Brewer's medium; BD) via intraperitoneal (IP) injection to recruit monocytes/macrophages). After 24 h, mice were infected with HCMV TB40/E-*UL136myc* or *UL136myc* mutant-infected fibroblasts (approximately 10^5 PFU per mouse) via IP injection. A control group of engrafted mice was mock infected using uninfected fibroblasts. The virus was reactivated as previously described (44, 75).

Quantitative PCR for viral genomes in huNSG mice

Total DNA was extracted from approximately 1 mm^2 sections of mouse spleen or liver using the DNAzol kit (Life Technologies), and processed as previously described (44). Primers and a probe-recognizing HCMV UL141 were used to quantify HCMV genomes (probe = CGAGGGAGAGCAAGTT; forward primer = 5′GATGTGGGCCGAGAATTATGA and reverse primer = 5′ATGGGCCAGGAGTGTGTCA). The reaction was initiated using TaqMan Fast Advanced Master Mix (Applied Biosystems) activated at 95°C for 10 min followed by 40 cycles (15 s at 95°C and 1 min at 60°C) using a StepOnePlus TaqMan PCR machine. Results were analyzed using ABI StepOne software.

ACKNOWLEDGMENTS

This study was supported by the National Institutes of Allergy and Infectious Diseases/National Institutes of Health (NIAID/NIH) grants AI079059 and AI127335 to F.G. and AI127335 awarded to P.C.

We are grateful for the support of the Flow Cytometry and Human Immune Monitoring Shared Resource, supported through the Cancer Center Support Grant P30 CA023074 awarded to the University of Arizona. We are grateful to Pierce Longmire for assistance with the SRA sequence submission.

We thank Drs. James Alwine (University of Pennsylvania) and Lynn Enquist (Princeton University) for critical discussions on this work. We are grateful to Dr. Emmanuel Katsanis for his assistance in coordinating medical waste use in these studies.

AUTHOR AFFILIATIONS

[1]Cancer Biology Graduate Interdisciplinary Program, University of Arizona, Tucson, Arizona, USA
[2]Department of Immunobiology, University of Arizona, Tucson, Arizona, USA
[3]BIO5 Institute, University of Arizona, Tucson, Arizona, USA
[4]Vaccine and Gene Therapy Institute, Oregon Health and Science University, Beaverton, Oregon, USA
[5]Graduate Interdisciplinary Program in Genetics, University of Arizona, Tucson, Arizona, USA

PRESENT ADDRESS

Melissa A. Moy, Imanis Life Sciences, Rochester, Minnesota, USA
Lindsey Crawford, Department of Biochemistry, University of Nebraska-Lincoln, Lincoln, Nebraska, USA
Katie Caviness, National Biodefense Analysis and Countermeasures Center, Fort Detrick, Maryland, USA

AUTHOR ORCIDs

Patrizia Caposio http://orcid.org/0000-0001-7579-849X
Felicia Goodrum http://orcid.org/0000-0002-6646-7290

FUNDING

Funder	Grant(s)	Author(s)
HHS | NIH | National Institute of Allergy and Infectious Diseases (NIAID)	AI079059	Felicia Goodrum
HHS | NIH | National Institute of Allergy and Infectious Diseases (NIAID)	AI127335	Felicia Goodrum
HHS | NIH | National Institute of Allergy and Infectious Diseases (NIAID)	AI127335	Patrizia Caposio

AUTHOR CONTRIBUTIONS

Melissa A. Moy, Conceptualization, Data curation, Formal analysis, Investigation, Methodology, Writing – original draft, Writing – review and editing | Donna Collins-McMillen, Data curation, Formal analysis, Investigation, Methodology, Writing – review and editing | Lindsey Crawford, Data curation, Formal analysis, Investigation, Methodology, Writing – review and editing | Christopher Parkins, Data curation, Formal analysis, Methodology | Sebastian Zeltzer, Conceptualization, Formal analysis, Writing – review and editing | Katie Caviness, Conceptualization, Writing – review and editing | Syed Shujaat Ali Zaidi, Data curation, visualization | Patrizia Caposio, Conceptualization, Data curation, Formal analysis, Investigation, Methodology, Writing – review and editing | Felicia Goodrum, Conceptualization, Data curation, Formal analysis, Funding acquisition, Investigation, Methodology, Project administration, Resources, Supervision, Writing – original draft, Writing – review and editing

DATA AVAILABILITY

Raw viral genome sequences read have been deposited in the Sequence Read Archive (SRA) (BioProject ID: PRJNA926319).

REFERENCES

1. Cannon MJ, Schmid DS, Hyde TB. 2010. Review of cytomegalovirus seroprevalence and demographic characteristics associated with infection. Rev Med Virol 20:202–213. https://doi.org/10.1002/rmv.655
2. Korndewal MJ, Mollema L, Tcherniaeva I, van der Klis F, Kroes ACM, Oudesluys-Murphy AM, Vossen ACTM, de Melker HE. 2015. Cytomegalovirus infection in the Netherlands: seroprevalence, risk factors, and implications. J Clin Virol 63:53–58. https://doi.org/10.1016/j.jcv.2014.11.033
3. Zuhair M, Smit GSA, Wallis G, Jabbar F, Smith C, Devleesschauwer B, Griffiths P. 2019. Estimation of the worldwide seroprevalence of cytomegalovirus: a systematic review and meta-analysis. Rev Med Virol 29:e2034. https://doi.org/10.1002/rmv.2034
4. Goodrum F, Britt W, Mocarski ES. 2021. Cytomegalovirus. In Whelan SPJ, EO Freed, L Enquist (ed), Fields virology, 7th ed, vol 2. DNA Viruses, Wolters Kluwer, Philadelphia, Baltimore, New York, London, Hong Kong, Buenos Aires, Sydney, Tokyo.
5. Britt W. 2008. Manifestations of human cytomegalovirus infection: proposed mechanisms of acute and chronic disease. Curr Top Microbiol Immunol 325:417–470. https://doi.org/10.1007/978-3-540-77349-8_23
6. Boeckh M. 2011. Complications, diagnosis, management, and prevention of CMV infections: current and future. Hematology Am Soc Hematol Educ Program 2011:305–309. https://doi.org/10.1182/asheducation-2011.1.305
7. Boeckh M, Geballe AP. 2011. Cytomegalovirus: pathogen, paradigm, and puzzle. J Clin Invest 121:1673–1680. https://doi.org/10.1172/JCI45449
8. Boeckh M, Leisenring W, Riddell SR, Bowden RA, Huang M-L, Myerson D, Stevens-Ayers T, Flowers MED, Cunningham T, Corey L. 2003. Late cytomegalovirus disease and mortality in recipients of allogeneic hematopoietic stem cell transplants: importance of viral load and T-cell immunity. Blood 101:407–414. https://doi.org/10.1182/blood-2002-03-0993
9. Britt WJ. 2018. Maternal immunity and the natural history of congenital human cytomegalovirus infection. Viruses 10:405. https://doi.org/10.3390/v10080405
10. Cannon MJ. 2009. Congenital cytomegalovirus (CMV) epidemiology and awareness. J Clin Virol 46:S6–S10. https://doi.org/10.1016/j.jcv.2009.09.002
11. Cannon MJ, Hyde TB, Schmid DS. 2011. Review of cytomegalovirus shedding in bodily fluids and relevance to congenital cytomegalovirus infection. Rev Med Virol 21:240–255. https://doi.org/10.1002/rmv.695
12. Britt WJ. 2020. Human cytomegalovirus infection in women with preexisting immunity: sources of infection and mechanisms of infection in the presence of antiviral immunity. J Infect Dis 221:S1–S8. https://doi.org/10.1093/infdis/jiz464
13. Anastasio ART, Yamamoto AY, Massuda ET, Manfredi AKS, Cavalcante JMS, Lopes BCP, Aragon DC, Boppana S, Fowler KB, Britt WJ, Mussi-Pinhata MM. 2021. Comprehensive evaluation of risk factors for neonatal hearing loss in a large Brazilian cohort. J Perinatol 41:315–323. https://doi.org/10.1038/s41372-020-00807-8
14. Krstanović F, Britt WJ, Jonjić S, Brizić I. 2021. Cytomegalovirus infection and inflammation in developing brain. Viruses 13:1078. https://doi.org/10.3390/v13061078
15. Zhou YP, Mei MJ, Wang XZ, Huang SN, Chen L, Zhang M, Li XY, Qin HB, Dong X, Cheng S, Wen L, Yang B, An XF, He AD, Zhang B, Zeng WB, Li XJ, Lu Y, Li HC, Li H, Zou WG, Redwood AJ, Rayner S, Cheng H, McVoy MA, Tang Q, Britt WJ, Zhou X, Jiang X, Luo MH. 2022. A congenital CMV infection model for follow-up studies of neurodevelopmental disorders, neuroimaging abnormalities, and treatment. JCI Insight 7:e152551. https://doi.org/10.1172/jci.insight.152551
16. Redeker A, Remmerswaal EBM, van der Gracht ETI, Welten SPM, Höllt T, Koning F, Cicin-Sain L, Nikolich-Žugich J, Ten Berge IJM, van Lier RAW, van Unen V, Arens R. 2017. The contribution of cytomegalovirus infection to immune senescence is set by the infectious dose. Front Immunol 8:1953. https://doi.org/10.3389/fimmu.2017.01953
17. Griffiths SJ, Riddell NE, Masters J, Libri V, Henson SM, Wertheimer A, Wallace D, Sims S, Rivino L, Larbi A, Kemeny DM, Nikolich-Zugich J, Kern F, Klenerman P, Emery VC, Akbar AN. 2013. Age-associated increase of low-avidity cytomegalovirus-specific CD8+ T cells that re-express CD45RA. J Immunol 190:5363–5372. https://doi.org/10.4049/jimmunol.1203267
18. Wertheimer AM, Bennett MS, Park B, Uhrlaub JL, Martinez C, Pulko V, Currier NL, Nikolich-Žugich D, Kaye J, Nikolich-Žugich J. 2014. Aging and cytomegalovirus infection differentially and jointly affect distinct circulating T cell subsets in humans. J Immunol 192:2143–2155. https://doi.org/10.4049/jimmunol.1301721
19. Goodrum F. 2022. The complex biology of human cytomegalovirus latency. Adv Virus Res 112:31–85. https://doi.org/10.1016/bs.aivir.2022.01.001
20. Hale AE, Collins-McMillen D, Lenarcic EM, Igarashi S, Kamil JP, Goodrum F, Moorman NJ. 2020. FOXO transcription factors activate alternative major immediate early promoters to induce human cytomegalovirus reactivation. Proc Natl Acad Sci U S A 117:18764–18770. https://doi.org/10.1073/pnas.2002651117
21. Min C-K, Shakya AK, Lee B-J, Streblow DN, Caposio P, Yurochko AD. 2020. The differentiation of human cytomegalovirus infected-monocytes is required for viral replication. Front Cell Infect Microbiol 10:368. https://doi.org/10.3389/fcimb.2020.00368
22. Krishna BA, Wass AB, O'Connor CM. 2020. Activator protein-1 transactivation of the major immediate early locus is a determinant of

cytomegalovirus reactivation from latency. Proc Natl Acad Sci U S A 117:20860–20867. https://doi.org/10.1073/pnas.2009420117
23. Zhang H, Domma AJ, Goodrum FD, Moorman NJ, Kamil JP, Shenk T. 2022. The Akt forkhead box O transcription factor axis regulates human cytomegalovirus replication. mBio 13:e0104222. https://doi.org/10.1128/mbio.01042-22
24. Hancock MH, Crawford LB, Perez W, Struthers HM, Mitchell J, Caposio P. 2021. Human cytomegalovirus UL7, miR-US5-1, and miR-UL112-3p inactivation of FOXO3a protects CD34$^+$ hematopoietic progenitor cells from apoptosis. mSphere 6:e00986-20. https://doi.org/10.1128/mSphere.00986-20
25. Crawford LB, Kim JH, Collins-McMillen D, Lee B-J, Landais I, Held C, Nelson JA, Yurochko AD, Caposio P. 2018. Human cytomegalovirus encodes a novel FLT3 receptor ligand necessary for hematopoietic cell differentiation and viral reactivation. mBio 9:e00682-18. https://doi.org/10.1128/mBio.00682-18
26. Goodrum F, Britt W, Mocarski ES. 2022. P. M. Howley, D. M. Knipe, J. L. Cohen, and B. A. Damania. Cytomegalovirus. 7th ed. Vol. 2. Fields Virology: DNA Viruses, Wolters Kluwer.
27. McAdams HH, Arkin A. 1998. Simulation of prokaryotic genetic circuits. Annu Rev Biophys Biomol Struct 27:199–224. https://doi.org/10.1146/annurev.biophys.27.1.199
28. Brophy JAN, Voigt CA. 2014. Principles of genetic circuit design. Nat Methods 11:508–520. https://doi.org/10.1038/nmeth.2926
29. Cha TA, Tom E, Kemble GW, Duke GM, Mocarski ES, Spaete RR. 1996. Human cytomegalovirus clinical isolates carry at least 19 genes not found in laboratory strains. J Virol 70:78–83. https://doi.org/10.1128/JVI.70.1.78-83.1996
30. Dolan A, Cunningham C, Hector RD, Hassan-Walker AF, Lee L, Addison C, Dargan DJ, McGeoch DJ, Gatherer D, Emery VC, Griffiths PD, Sinzger C, McSharry BP, Wilkinson GWG, Davison AJ. 2004. Genetic content of wild-type human cytomegalovirus. J Gen Virol 85:1301–1312. https://doi.org/10.1099/vir.0.79888-0
31. Murphy E, Rigoutsos I, Shibuya T, Shenk TE. 2003. Reevaluation of human cytomegalovirus coding potential. Proc Natl Acad Sci U S A 100:13585–13590. https://doi.org/10.1073/pnas.1735466100
32. Murphy E, Shenk T. 2008. Human cytomegalovirus genome. Curr Top Microbiol Immunol 325:1–19. https://doi.org/10.1007/978-3-540-77349-8_1
33. Murphy E, Yu D, Grimwood J, Schmutz J, Dickson M, Jarvis MA, Hahn G, Nelson JA, Myers RM, Shenk TE. 2003. Coding potential of laboratory and clinical strains of human cytomegalovirus. Proc Natl Acad Sci U S A 100:14976–14981. https://doi.org/10.1073/pnas.2136652100
34. Umashankar M, Petrucelli A, Cicchini L, Caposio P, Kreklywich CN, Rak M, Bughio F, Goldman DC, Hamlin KL, Nelson JA, Fleming WH, Streblow DN, Goodrum F. 2011. A novel human cytomegalovirus locus modulates cell type-specific outcomes of infection. PLoS Pathog 7:e1002444. https://doi.org/10.1371/journal.ppat.1002444
35. Dutta N, Lashmit P, Yuan J, Meier J, Stinski MF. 2015. The human cytomegalovirus UL133-138 gene locus attenuates the lytic viral cycle in fibroblasts. PLoS One 10:e0120946. https://doi.org/10.1371/journal.pone.0120946
36. Wang W, Taylor SL, Leisenfelder SA, Morton R, Moffat JF, Smirnov S, Zhu H. 2005. Human cytomegalovirus genes in the 15-kilobase region are required for viral replication in implanted human tissues in SCID mice. J Virol 79:2115–2123. https://doi.org/10.1128/JVI.79.4.2115-2123.2005
37. Kempová V, Lenhartová S, Benko M, Nemčovič M, Kúdelová M, Nemčovičová I. 2020. The power of human cytomegalovirus (HCMV) hijacked UL/B' functions lost *in vitro*. Acta Virol 64:117–130. https://doi.org/10.4149/av_2020_202
38. Mlera L, Moy M, Maness K, Tran LN, Goodrum FD. 2020. The role of the human cytomegalovirus *UL133-UL138* gene locus in latency and reactivation. Viruses 12:714. https://doi.org/10.3390/v12070714
39. Petrucelli A, Rak M, Grainger L, Goodrum F. 2009. Characterization of a novel Golgi apparatus-localized latency determinant encoded by human cytomegalovirus. J Virol 83:5615–5629. https://doi.org/10.1128/JVI.01989-08
40. Umashankar M, Rak M, Bughio F, Zagallo P, Caviness K, Goodrum FD. 2014. Antagonistic determinants controlling replicative and latent states of human cytomegalovirus infection. J Virol 88:5987–6002. https://doi.org/10.1128/JVI.03506-13
41. Li G, Rak M, Nguyen CC, Umashankar M, Goodrum FD, Kamil JP. 2014. An Epistatic relationship between the viral protein kinase UL97 and the *UL133-UL138* latency locus during the human cytomegalovirus lytic cycle. J Virol 88:6047–6060. https://doi.org/10.1128/JVI.00447-14
42. Wang D, Li G, Schauflinger M, Nguyen CC, Hall ED, Yurochko AD, von Einem J, Kamil JP. 2013. The ULb' region of the human cytomegalovirus genome confers an increased requirement for the viral protein kinase UL97. J Virol 87:6359–6376. https://doi.org/10.1128/JVI.03477-12
43. Caviness K, Cicchini L, Rak M, Umashankar M, Goodrum F. 2014. Complex expression of the UL136 gene of human cytomegalovirus results in multiple protein isoforms with unique roles in replication. J Virol 88:14412–14425. https://doi.org/10.1128/JVI.02711-14
44. Caviness K, Bughio F, Crawford LB, Streblow DN, Nelson JA, Caposio P, Goodrum F. 2016. Complex interplay of the *UL136* isoforms balances cytomegalovirus replication and latency. mBio 7:e01986. https://doi.org/10.1128/mBio.01986-15
45. Mlera L, Zeltzer S, Collins-McMillen D, Buehler JC, Moy M, Caviness K, Cicchini L, Goodrum F. 2022. LXR-inducible host E3 Ligase IDOL targets a human cytomegalovirus reactivation determinant to promote latency. bioRxiv. https://doi.org/10.1101/2022.11.15.516687:2022.11.15.516687
46. McSharry BP, Tomasec P, Neale ML, Wilkinson GWG. 2003. The most abundantly transcribed human cytomegalovirus gene (beta 2.7) is non-essential for growth *in vitro*. J Gen Virol 84:2511–2516. https://doi.org/10.1099/vir.0.19298-0
47. Collins-McMillen D, Rak M, Buehler JC, Igarashi-Hayes S, Kamil JP, Moorman NJ, Goodrum F. 2019. Alternative promoters drive human cytomegalovirus reactivation from latency. Proc Natl Acad Sci U S A 116:17492–17497. https://doi.org/10.1073/pnas.1900783116
48. Fehr AR, Yu D. 2011. Human cytomegalovirus early protein pUL21A promotes efficientviral DNA synthesis and the late accumulation of immediate-early transcripts. J Virol 85:663–674. https://doi.org/10.1128/JVI.01599-10
49. Camus S, Menéndez S, Cheok CF, Stevenson LF, Laín S, Lane DP. 2007. Ubiquitin-independent degradation of p53 mediated by high-risk human papillomavirus protein E6. Oncogene 26:4059–4070. https://doi.org/10.1038/sj.onc.1210188
50. Erales J, Coffino P. 2014. Ubiquitin-independent proteasomal degradation. Biochim Biophys Acta 1843:216–221. https://doi.org/10.1016/j.bbamcr.2013.05.008
51. Hwang J, Kalejta RF. 2007. Proteasome-dependent, ubiquitin-independent degradation of Daxx by the viral pp71 protein in human cytomegalovirus-infected cells. Virology 367:334–338. https://doi.org/10.1016/j.virol.2007.05.037
52. Kalejta RF, Shenk T. 2003. Proteasome-dependent, ubiquitin-independent degradation of the Rb family of tumor suppressors by the human cytomegalovirus pp71 protein. Proc Natl Acad Sci U S A 100:3263–3268. https://doi.org/10.1073/pnas.0538058100
53. Winkler LL, Hwang J, Kalejta RF. 2013. Ubiquitin-independent proteasomal degradation of tumor suppressors by human cytomegalovirus pp71 requires the 19S regulatory particle. J Virol 87:4665–4671. https://doi.org/10.1128/JVI.03301-12
54. Peppenelli M, Buehler J, Goodrum F. 2021. Human hematopoietic long-term culture (hLTC) for human cytomegalovirus latency and reactivation. Methods Mol Biol 2244:83–101. https://doi.org/10.1007/978-1-0716-1111-1_5
55. Rak MA, Buehler J, Zeltzer S, Reitsma J, Molina B, Terhune S, Goodrum F. 2018. Human cytomegalovirus UL135 interacts with host adaptor proteins to regulate epidermal growth factor receptor and reactivation from latency. J Virol 92:e00919-18. https://doi.org/10.1128/JVI.00919-18
56. Stern-Ginossar N, Weisburd B, Michalski A, Le VTK, Hein MY, Huang S-X, Ma M, Shen B, Qian S-B, Hengel H, Mann M, Ingolia NT, Weissman JS. 2012. Decoding human cytomegalovirus. Science 338:1088–1093. https://doi.org/10.1126/science.1227919
57. Grainger L, Cicchini L, Rak M, Petrucelli A, Fitzgerald KD, Semler BL, Goodrum F. 2010. Stress-inducible alternative translation initiation of human cytomegalovirus latency protein pUL138. J Virol 84:9472–9486. https://doi.org/10.1128/JVI.00855-10
58. Schommartz T, Tang J, Brost R, Brune W. 2017. Differential requirement of human cytomegalovirus UL112-113 protein isoforms for viral replication. J Virol 91:e00254-17. https://doi.org/10.1128/JVI.00254-17

59. Isomura H, Stinski MF, Kudoh A, Murata T, Nakayama S, Sato Y, Iwahori S, Tsurumi T. 2008. Noncanonical TATA sequence in the UL44 late promoter of human cytomegalovirus is required for the accumulation of late viral transcripts. J Virol 82:1638–1646. https://doi.org/10.1128/JVI.01917-07
60. Kerry JA, Priddy MA, Kohler CP, Staley TL, Weber D, Jones TR, Stenberg RM. 1997. Translational regulation of the human cytomegalovirus pp28 (UL99) late gene. J Virol 71:981–987. https://doi.org/10.1128/JVI.71.2.981-987.1997
61. Seo J-Y, Britt WJ. 2006. Sequence requirements for localization of human cytomegalovirus tegument protein pp28 to the virus assembly compartment and for assembly of infectious virus. J Virol 80:5611–5626. https://doi.org/10.1128/JVI.02630-05
62. Wakeman BS, Izumiya Y, Speck SH. 2017. Identification of novel Kaposi's sarcoma-associated herpesvirus *orf50* transcripts: discovery of new RTA Isoforms with variable transactivation potential. J Virol 91:e01434-16. https://doi.org/10.1128/JVI.01434-16
63. Reuven NB, Antoku S, Weller SK. 2004. The UL12.5 gene product of herpes simplex virus type 1 exhibits nuclease and strand exchange activities but does not localize to the nucleus. J Virol 78:4599–4608. https://doi.org/10.1128/jvi.78.9.4599-4608.2004
64. Bughio F, Umashankar M, Wilson J, Goodrum F. 2015. Human cytomegalovirus *UL135* and *UL136* genes are required for postentry tropism in endothelial cells. J Virol 89:6536–6550. https://doi.org/10.1128/JVI.00284-15
65. Michel D, Pavić I, Zimmermann A, Haupt E, Wunderlich K, Heuschmid M, Mertens T. 1996. The Ul97 gene product of human cytomegalovirus is an early-late protein with a nuclear localization but is not a nucleoside kinase. J Virol 70:6340–6346. https://doi.org/10.1128/JVI.70.9.6340-6346.1996
66. Buehler J, Zeltzer S, Reitsma J, Petrucelli A, Umashankar M, Rak M, Zagallo P, Schroeder J, Terhune S, Goodrum F. 2016. Opposing regulation of the EGF receptor: a molecular switch controlling cytomegalovirus latency and replication. PLoS Pathog 12:e1005655. https://doi.org/10.1371/journal.ppat.1005655
67. Buehler J, Carpenter E, Zeltzer S, Igarashi S, Rak M, Mikell I, Nelson JA, Goodrum F. 2019. Host signaling and EGR1 transcriptional control of human cytomegalovirus replication and latency. PLoS Pathog 15:e1008037. https://doi.org/10.1371/journal.ppat.1008037
68. Smith NA, Chan GC, O'Connor CM. 2021. Modulation of host cell signaling during cytomegalovirus latency and reactivation. Virol J 18:207. https://doi.org/10.1186/s12985-021-01674-1
69. Stanton RJ, Prod'homme V, Purbhoo MA, Moore M, Aicheler RJ, Heinzmann M, Bailer SM, Haas J, Antrobus R, Weekes MP, Lehner PJ, Vojtesek B, Miners KL, Man S, Wilkie GS, Davison AJ, Wang ECY, Tomasec P, Wilkinson GWG. 2014. HCMV pUL135 remodels the actin cytoskeleton to impair immune recognition of infected cells. Cell Host Microbe 16:201–214. https://doi.org/10.1016/j.chom.2014.07.005
70. Ferrell JE, Ha SH. 2014. Ultrasensitivity part III: cascades, bistable switches, and oscillators. Trends Biochem Sci 39:612–618. https://doi.org/10.1016/j.tibs.2014.10.002
71. Sinzger C, Hahn G, Digel M, Katona R, Sampaio KL, Messerle M, Hengel H, Koszinowski U, Brune W, Adler B. 2008. Cloning and sequencing of a highly productive, endotheliotropic virus strain derived from human cytomegalovirus TB40/E. J Gen Virol 89:359–368. https://doi.org/10.1099/vir.0.83286-0
72. Warming S, Costantino N, Court DL, Jenkins NA, Copeland NG. 2005. Simple and highly efficient BAC recombineering using *galK* selection. Nucleic Acids Res 33:e36. https://doi.org/10.1093/nar/gni035
73. Yu D, Ellis HM, Lee EC, Jenkins NA, Copeland NG, Court DL. 2000. An efficient recombination system for chromosome engineering in *Escherichia coli*. Proc Natl Acad Sci U S A 97:5978–5983. https://doi.org/10.1073/pnas.100127597
74. Hu Y, Smyth GK. 2009. ELDA: extreme limiting dilution analysis for comparing depleted and enriched populations in stem cell and other assays. J Immunol Methods 347:70–78. https://doi.org/10.1016/j.jim.2009.06.008
75. Smith MS, Goldman DC, Bailey AS, Pfaffle DL, Kreklywich CN, Spencer DB, Othieno FA, Streblow DN, Garcia JV, Fleming WH, Nelson JA. 2010. Granulocyte-colony stimulating factor reactivates human cytomegalovirus in a latently infected humanized mouse model. Cell Host Microbe 8:284–291. https://doi.org/10.1016/j.chom.2010.08.001